Calibration of a low cost 2D laser scanner

JIAWEI ZHANG
February 2016

SUPERVISORS:
Prof.dr.ir. M.G. Vosselman
Dr. M.S. Peter

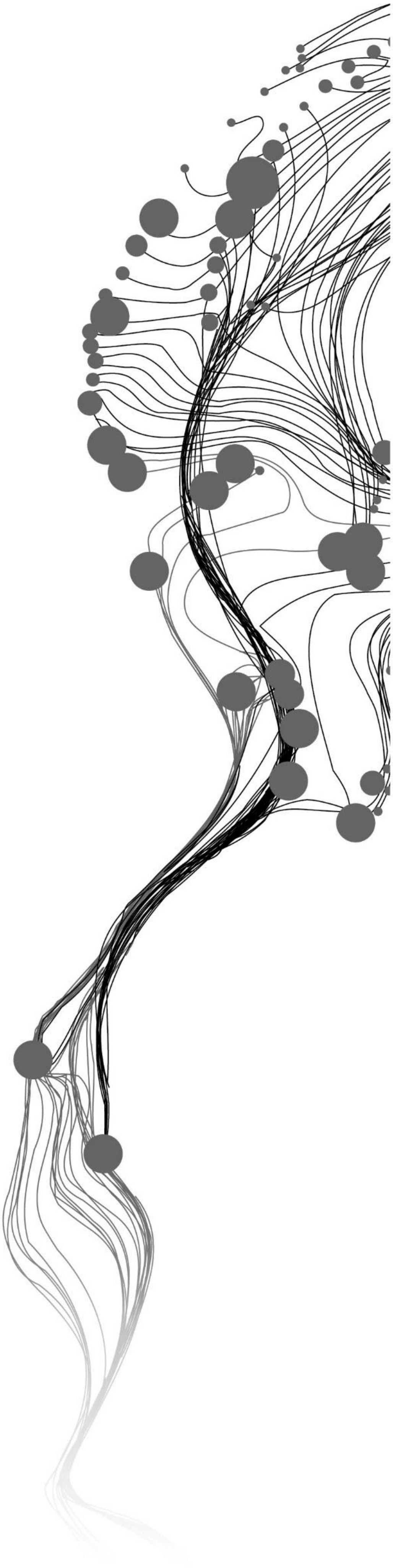

Calibration of a low cost 2D laser scanner

JIAWEI ZHANG

Enschede, The Netherlands, February, 2016

Thesis submitted to the Faculty of Geo-Information Science and Earth Observation of the University of Twente in partial fulfilment of the requirements for the degree of Master of Science in Geo-information Science and Earth Observation.
Specialization: Geoinformatics

SUPERVISORS:
Prof.dr.ir. M.G. Vosselman
Dr. M.S. Peter

THESIS ASSESSMENT BOARD:
Prof.dr.ir. A. Stein (Chair)
Dr. R.C. Lindenbergh (External Examiner, Delft University of Technology, Optical and Laser Remote Sensing)

DISCLAIMER

ABSTRACT

The main objective of my M.Sc. research is to formulate a calibration model for a low-cost 2D laser scanner and evaluate its accuracy.

The methodology is divided into 3 main steps: step 1 is pre-process data, in where both of the reference data and laser data have been prepared for the future calculation. Step 2 is to get the coordinates of measured points in model coordinate system using least square with the approximate values of rotation of the laser scanner, coordinates of the scanner in model coordinate system. With those coordinates of measured points, the plot of measured points and reference data can be drawn, through which, the systematic error can be seen and the calibration parameter then has been added. Another calibration parameter has been added after iterating above process. The last step is noise analysis, which is to analyze the accuracy over range and accuracy over time.

The proposed calibration model has successfully improved the accuracy of the laser scanner. The accuracy of the calibrated laser scanner is around 0.7cm, which is way below its guaranteed accuracy 3cm.

Keywords

2D laser scanner, calibration model, noise analysis, accuracy.

ACKNOWLEDGEMENTS

I would like to take this opportunity to express my gratitude to the people who helped me with my research during my stay in ITC, university of Twente, Enschede, the Netherlands.

First of all, I want to thank my supervisors Prof.dr.ir. M.G. Vosselman and Dr. M.S. Peter for the help and dedication to my research, especially my first supervisor Prof. Vosselman, who gave me very clear instructions during my research and he always provided me with very accurate answers whenever I met problems in coding, analyzing and writing, he elaborated thoroughly and vividly the things that I didn't understand. Besides that, he has also impressed me with his good personality, he is very nice and patient with me and my research.

Also I want to thank Dr. S.R.U.N. Jafri and Mr. A.S. Masselink for providing their help when acquiring the data for the research.

I want to thank my parents for supporting me, words cannot express how I love you both and the appreciation of your support for me studying in the Netherlands.

I want to thank my friends from GFM course, who brought the joy and happiness to me, especially thanks to Na Jin, Jiatan Jiang, Yizhen Lao, Wanpeng Shao, Jianwei Pan, Yancheng Wang, Yalda Saedi, Asgan Riza Nasrullah and so on.

I also want to thank the friends from other than GFM course, we had a lot of fun despite we never took a class together, especially goes to Yifei Xue, Yuangen Jiang, Xianghuan Luo, Julinda Dyli, Analia Guachalla Terrazas, Maurice Mugabowindekwe .etc. And my thanks go to the friends from previous year who gave me guidance and help for me living and studying here, especially Xiaoxu Li and Lingyue Kong.

Jiawei Zhang
Feb 2016

TABLE OF CONTENTS

1. Introduction 7

1.1 Motivation 7

1.2 Research problem 7

1.3 Research objectives 8

1.4 Research questions 8

1.5 Anticipated results 8

1.6. Thesis structure 8

2 Literature Review 9

2.1 Measurement principle of laser scanner 9

2.2 Indoor mapping 10

2.3 Calibration of laser scanner 11

2.4 Summary 14

3 Methodology 15

3.1 Framework 15

3.2 Data collection 15

3.3 Formulation of mathematical model 18

4 Implementation and analysis 24

4.1 Specification of scanner 24

4.2 Pre-process data 25

4.3 Convergence 26

4.4 Plots 27

4.5 RMS 34

4.6 Proposed calibration model 36

4.7 Noise analysis after calibration 37

5 Evaluation and discussion 43

5.1 Evaluation 43

5.2 Discussion 43

6 Conclusion 45

6.1 Conclusions 45

6.2 Answers to the research questions. 45

6.3 Recommendations 46

List of References 47

LIST OF FIGURES

Figure 1- 1 Design of the scanning system (Vosselman, 2014) 7
Figure 2- 1 Measurement principle of light transit time (Vosselman & Maas, 2010) 9
Figure 2- 2 Measurement principle based on CW using AM (NRC Crown copyright) 9
Figure 2- 3 Measurement principle based on CW using AM (NRC Crown copyright) 10
Figure 2- 4 Measurement principle of triangulation (Vosselman & Maas, 2010) 10
Figure 2- 5 Experiment setup for Sick LMS 200 (Ye & Borenstein, 2002) 11
Figure 2- 6 Experiment setup for Infrared Range Finder PBS-03JN (Kim, J. B., & Kim, B. K. ,2011) 12
Figure 2- 7 Geometric model (Mader et al., 2014) 13
Figure 2- 8 Location of laser i on the plate (Sheehan et al., 2012) 13
Figure 2- 9 An indoor environment created by the calibrated scanning system (Sheehan et al., 2012) 14
Figure 3- 1 Flowchart of the methodology 15
Figure 3- 2 Chosen indoor environment 16
Figure 3- 3 Plan of the indoor environment 16
Figure 3- 4 Obstacles at corner in the indoor environment 16
Figure 3- 5 Measurement of the indoor environment using tape 17
Figure 3- 6 Illustration of the locally defined coordinate system 18
Figure 4- 1 Hokuyo UTM-30LX (Hokuyo Ltd, 2012) 24
Figure 4- 2 Structure of the laser scanner (Hokuyo Ltd, 2012) 24
Figure 4- 3 Labeling the measured points with corresponding walls 26
Figure 4- 4 Plot with the approximate values 28
Figure 4- 5 Plot after 1st step 28
Figure 4- 6 Enlargement of residuals after 1st step 29
Figure 4- 7 Plot after 2nd step 29
Figure 4- 8 Enlargement of residuals after 2nd step 30
Figure 4- 9 Plot after 3rd step 30
Figure 4- 10 Enlargement of residual 10 times for data 2-1 of the corner of classroom 31
Figure 4- 11 Plot with approximate values 31
Figure 4- 12 Plot after 1st step 32
Figure 4- 13 Enlargement of residuals after 1st step 32
Figure 4- 14 Plot after 2nd step 33
Figure 4- 15 Enlargement of residuals after 2nd step 33
Figure 4- 16 Plot after 3rd step 34
Figure 4- 17 Enlargement of residual 10 times for data 5-1 of the center of classroom 34
Figure 4- 18 Illustration of calculation of the RMS on range 35
Figure 4- 19 Mean absolute values of residuals on range for data 2-1, 5-1, 10-1 of the corner of classroom 37
Figure 4- 20 Standard deviation of residuals on range for data 2-1, 5-1, 10-1 of the corner of classroom 38
Figure 4- 21 Mean absolute values of residuals on range for data 2-1, 5-1, 10-1 of the center of classroom 38

Figure 4- 22 Standard deviation of residuals on range for data 2-1, 5-1, 10-1 of the center of classroom 38
Figure 4- 23 Labeling data acquired at the corner 39
Figure 4- 24 Labeling data acquired at the center 40
Figure 4- 25 Plot of calibrated scanner with data acquired on earlier time 42
Figure 4- 26 Mean value of residual after calibration in dataset acquired earlier 42
Figure 6- 1 Enlargement of residual 10 times for data 5-1 of the center of classroom 46

LIST OF TABLES

Table 4- 1 Measured lengths in the triangle ACD, ABD 25
Table 4- 2 Measured lengths in the triangle CDF, CEF 25
Table 4- 3 Measured lengths in the triangle BGH, ABG 25
Table 4- 4 Measured lengths of wall 2 and wall 3 25
Table 4- 5 Lengths of each wall in the classroom 25
Table 4- 6 Values for β, X0 and Y0 in the data 2-1 of the data acquired at the corner 27
Table 4- 7 Values for β, X0 and Y0 in the data 5-1 of the data acquired at the center 27
Table 4- 8 Values of RMS and added parameters of data 2-1 of the corner of classroom 35
Table 4- 9 Values of RMS and added parameters of data 5-1 of the center of classroom 35
Table 4- 10 Values for parameters of calibration model of data acquired at the corner 36
Table 4- 11 Values for parameters of calibration model of data acquired at the center 36
Table 4- 12 Mean and standard deviation of scale k and offset i of data acquired at the corner .. 37
Table 4- 13 Mean and standard deviation of scale k and offset i of data acquired at the center ... 37
Table 4- 14 The number of points in each interval in 2 datasets 38
Table 4- 15 RMS and parameters of calibration model for dataset acquired at corner 40
Table 4- 16 Changes in RMS and RMS on range for dataset acquired at corner 40
Table 4- 17 RMS and parameters of calibration model for data acquired at the center 41
Table 4- 18 Changes in RMS and RMS on range for data acquired at the center 41
Table 4- 19 Comparison between data acquired on 2 different dates 41
Table 5- 1 RMS values of data acquired at the corner of classroom 43
Table 5- 2 RMS values of data acquired at the center of classroom 43

1. INTRODUCTION

1.1 Motivation

Laser scanning is widely used in the areas like surveying, manufacturing and construction. Laser scanners can get a huge number of points of target in a very short time, however, they are not always as accurate as manufacturers claim, even if they are, calibrating the laser scanner can improve the accuracy of measurement. Therefore, testing the accuracy of the laser scanner is very necessary in order to have a better results in the future scanning.

The accuracy of measurement using the laser scanning system may be influenced by random errors and systematic errors. Random errors cannot be calibrated because they don't have a pattern while systematic errors have a pattern which can be calibrated.

The errors may vary with the time of using the scanner and the range between the sensor and target. Time may influence the accuracy because when we use the scanners for a long time, the processing unit of the scanner might be influenced because of overheating. The distance between the sensor and target may influence the accuracy because the laser scanner may start receiving weaker signals when the distance is too large and the systematic errors may also change with range.

Calibration of laser scanner will eliminate the effect of systematic errors and create more accurate scanning results.

1.2 Research problem

In 2014, Vosselman designed an indoor mapping system using three 2D laser scanners. The pose of the system and the planes of floor, ceiling and walls can be reconstructed simultaneously. The reason for choosing 2D scanner instead of 3D is that 2D scanners are much cheaper than 3D scanners. Here is the design of the system: the three scanners are mounted with 270 degrees open angle, the top scanner scans in approximately horizontal plane while the other scanners are placed at an angle of 45 degrees with the moving direction and they are tilted by 45 degrees (Vosselman, 2014).

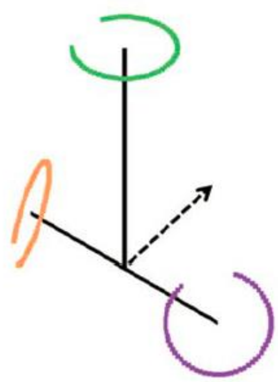

Figure 1- 1 Design of the scanning system (Vosselman, 2014)

The system are comprised of three cheap 2D laser scanners, 2D laser scanner may not be as accurate a 3D scanner, so it is necessary to do the calibration for the 2D laser scanners to improve their accuracy. The calibration of the laser scanners will have huge influence on this laser scanning system and the calibrated range measurement is also good for the registration of the scanning system and other procedures in using the system.

I am going to study what factors can influence the accuracy of measurement and formulate the mathematical models which can calibrate the systematic errors in the range measurement. I am going to figure out how to determine the error of range measurement using data generated by one of laser scanners. In other words, my research will be to calibrate the scanner in order to understand the accuracy potential and the stability of the range measurement over time.

1.3 Research objectives

1. Establish the mathematical model for the calibration of the scanning system.
2. Determine a configuration of an indoor space and a set of static scans that enables the calibration.
3. Improve the configuration such that the calibration accuracy meets a certain accuracy standard.
4. Analyze the noise after the calibration of the laser scanner.

1.4 Research questions

1. What is an appropriate indoor environment for calibration and how to determine if the scanner needs calibration?
2. What is the optimal mathematical model to calibrate the scanner?
3. How does the accuracy change with the range?
4. Is the calibration model stable? Are the values for the parameters stable or should I calibrate the scanner every time I use this?
5. How to evaluate the noise after calibration?

1.5 Anticipated results

The anticipated results are the determination of the indoor space allowing the calibration, the mathematical model for the calibration and the evaluation of the noise after calibration.

1.6. Thesis structure

Chapter 2 reviews the literature of the related work of principle of laser scanning, indoor mapping and laser scanner calibration. Chapter 3 describes the methodology of the calibration. Chapter 4 describes the implementation of the method and analysis of the results. Chapter 5 evaluates and discusses the performance of the method. Chapter 6 gives the conclusion and recommendation.

2 LITERATURE REVIEW

In this chapter, the work related to this topic has been introduced. Section 2.1 describes the measurement principle of laser scanner. Section 2.2 describes the indoor mapping and section 2.3 describes the calibration of laser scanner.

2.1 Measurement principle of laser scanner

There are 3 major active methods to measure using laser scanner, discrete pulse time of flight, phase measurements in continuous modulated waves and triangulation.

Light wave travels in a known velocity, knowing the time difference between the signal emits and receives allows calculating the distance between the sensor and target. Light transit time estimation can also be called as time-of-flight or lidar (light detection and ranging). The distance can be calculated as:

$$Z = c * delay/2 \tag{2.1}$$

Where Z is the distance, c is the velocity of light, delay is the time signal travels from emits to receives.

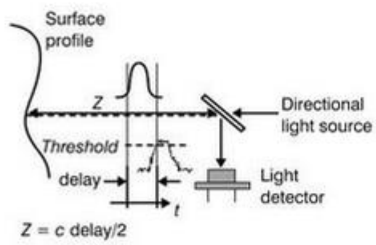

Figure 2- 1 Measurement principle of light transit time (Vosselman & Maas, 2010)

The distance can also be calculated using phase measurement in continuous wave (CW), which comprises of using amplitude modulation (AM) or frequency modulation (FM). AM uses the phase difference, the intensity of the laser is amplitude modulated, the emitted laser and collected laser beam are compared. Through the phase difference between two waves can we get the time delay.

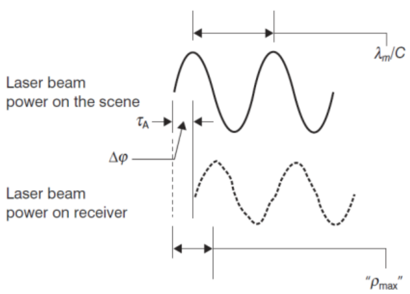

Figure 2- 2 Measurement principle based on CW using AM (NRC Crown copyright)

FM uses beat frequencies, phase-coded compression. The frequency of the laser beam is linearly modulated at the laser diode or with a modulator. The linear modulation is usually shaped as a triangular or a chirp. In this method, the important parts are determined by the coherent detection and beat frequency.

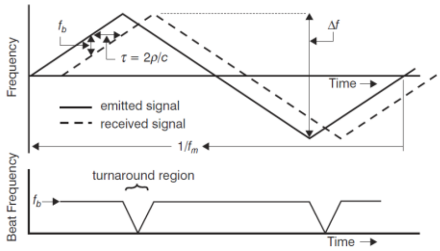

Figure 2- 3 Measurement principle based on CW using AM (NRC Crown copyright)

Triangulation uses cosine law in a constructed triangle which comprised by the distance between source and receiver (baseline), angle between source direction and baseline, angle between observation direction and baseline. The distance can be calculated as:

$$Z = B/(\tan\alpha + \tan\beta) \quad (2.2)$$

Where Z is the distance between laser scanner and target, B is the length of baseline, α is the angle between directional light source direction and target, β is the angle between observation direction and target (Vosselman & Maas, 2010).

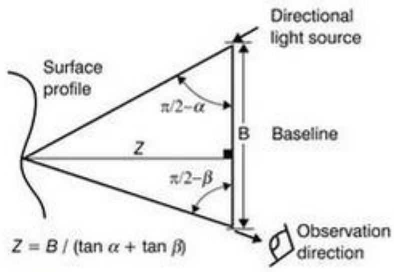

Figure 2- 4 Measurement principle of triangulation (Vosselman & Maas, 2010)

2.2 Indoor mapping

In 2003, Surmann et al., presented an automatic system to digitalize 3D indoor environments, which consists of a mobile robot with 3D laser range finder and three software modules including the registration of the data, computation of next nominal pose and stable motor controller. Another method to acquire 3D model of indoor office environments has been proposed by Biber et al., (2004). This method uses a mobile robot equipped with a 2D laser scanner to solve the SLAM problem and extract walls, it uses the data from a panoramic camera to extract textures, and multi-resolution blending to hide seams in the generated textures. Range camera can also be used to map an indoor environment, like Microsoft's Kinect sensor, which captures depth and color images at the same time, the integration of depth and color data gives us a colored point cloud. A complete point cloud of an indoor environment can be created by registering the depth images (Khoshelham & Elberink, 2012). Henry et al (2012) proposed an indoor mapping method using Kinect-style depth cameras, in where they used an optimization algorithm combing both visual features and shape-based alignment.

Despite range camera can quickly capture the points of target in 3D, it has a limited field of view and short range measurement which cannot be used in larger indoor environment. Therefore, in

2014, Vosselman designed a mapping system comprised of three 2D laser scanners without need for IMU. He also proposed a method to process range measurement so the pose of the system and the planes of floor, ceiling and walls can be simultaneously estimated. Instead of traditional scan line matching, the method predicts the transformation of the next scan lines and associates the scan line to the earlier reconstructed surfaces (Vosselman, 2014).

2.3 Calibration of laser scanner

There are 2 major categories of methods in calibrating a scanning system: first one is to use a reference directly to have a more accurate calibration and second one is self-calibration which uses network geometry to indirectly provide the reference, self-calibration is time-saving and doesn't require special equipment (Mader et al., 2014).

2.3.1 Calibration using references

For the first categories of methods, Ye & Borenstein proposed a method to calibrate Sick LMS 200 laser scanner through extensive experiments in 2002. They focused on the different parameters that are relevant to 3D mapping using this 2D laser scanner, which are data transfer rate, surface of the target, drift and incidence angle. They used a 4-meter linear motion table which was driven by a computer controlled motor to put the target from a specific distance to the scanner.

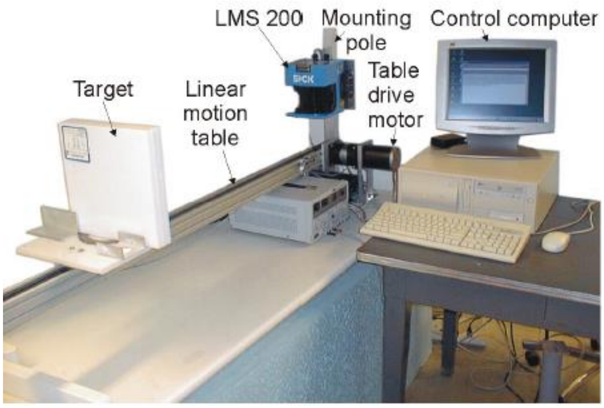

Figure 2- 5 Experiment setup for Sick LMS 200 (Ye & Borenstein, 2002)

However, Sick laser scanner has the problems of larger size, weight and power consuming while Hokuyo is less weighed and less power consuming. In order to investigate whether Hokuyo is as accurate as Sick, Okubo et al., tested the performance of 2 scanners under the same condition and proposed a calibration method in 2009. In both papers, they proposed a calibration model as:

$$\hat{y} = k\mu + b \tag{2.3}$$

In where $\hat{y}$ is the estimate of true distances y, μ is the mean of measured ranges, k is the scale constant, b is the offset constant for minimizing the square error.

Similar experiment has also been conducted by Kneip et al., (2009), who analyzed the characteristics of a Hokuyo model from aspects of general effects, drift effect, the influence of the sensor's spatial orientation, influence of missing ambient light, surface properties, distance and incidence angle. Their proposed calibration model relies on a simple polynomial regression of the third degree on the measured range.

Also, a calibration method using cubic hermite has been proposed by Kim & Kim in 2011, they use cubic hermite because of its continuity, smoothness and monotonicity in data regression, in where they proposed a calibration function which can minimize the error based on both distance and scan angle. They used white wall as their target because it is the most common target in indoor mapping, and they changed the distances and scan angle in a certain interval to obtain better error statistics.

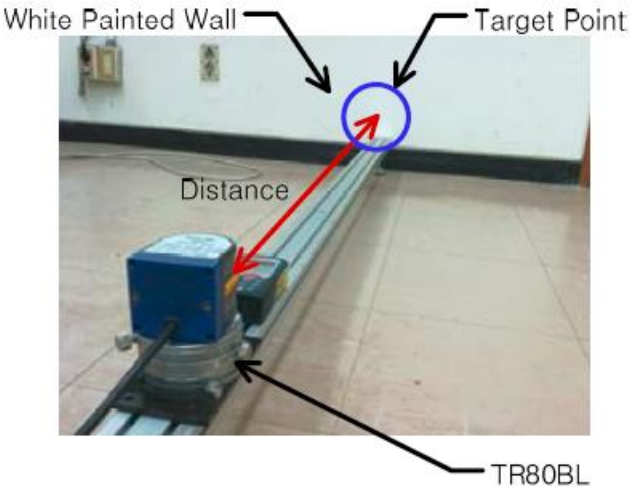

Figure 2- 6 Experiment setup for Infrared Range Finder PBS-03JN (Kim, J. B., & Kim, B. K. ,2011)

With the measured distance data at every scan angle have been approximated by cubic hermite spline. They have obtained the scan-wise cubic hermite splines as follows:

$$f_{i,j}(x) = a_{i,j}(x - x_{i,j})^3 + b_{i,j}(x - x_{i,j})^2 + c_{i,j}(x - x_{i,j}) + r_{i,j} \tag{2.4}$$

Where i is the distance interval, j is the angle interval, a, b, c are the coefficients for the function. In 2011, Jain et al., proposed a calibration method using frequency domain and time domain techniques, which can model the noises in the sensor while traditional methods like sample mean or variance cannot. They modeled the error using a combination of power-law noises with a spectral density form in the frequency domain technique, then use time domain technique to determine the parameters. They also used appropriate stochastic processes to model the random errors.

2.3.2 Self-calibration

As for the self-calibration methods, advantages are more redundancies using this method and no need to place signalized targets (Vosselman & Maas, 2010).

In 2010, Glennie & Lichti proposed a method using a planar feature-based least squares adjustment which can be used in a minimally constrained network, this method selected planar features as the targeted objects. In the method, the coefficients of the planes are estimated with the estimation of scanner position, orientation and calibration parameters. Because there are no targets with known locations, the scan network have been constrained by fixing an additional scan location. The use of their adjusted parameters has reduced in the planar misclosure RMSE.

A flexible method which needs a camera but doesn't need spatial object data has been proposed by Mader et al., in 2014, this method is more time saving because it doesn't need to determine the reference distances and it can jointly adjusts distance and angular data form laser scanner and the images from the camera, also can automatically estimate the observation weights. They have integrated all the necessary of observations and constraints in a joint functional and stochastic context. The geometric principle is based on a self-calibrating bundle adjustment of distance measurements with direction. They have proposed the model in the vertical and horizontal directions separately:

The appropriate distance correction model for vertical direction they use is:

$$\Delta D = a_0 + a_1 \cdot D \quad (2.5)$$

Where D is the distance error, ΔD is the correction to the distance error.

$$\Delta\alpha = b_1 \cdot \alpha + b_2 \cdot sin\alpha + b_3 \cdot cos\alpha + b_4 \cdot sin\, 2\alpha + b_5 \cdot cos\, 2\alpha + b_6 \cdot D^{-1} \quad (2.6)$$

Where b1 is a scale error, b2, b3 are for modeling the horizontal circle eccentricity, b4, b5 are for modeling the non-orthogonality of the plane. b6 describes the eccentricity of collimation axis relative to the rotation axis.

This method also needs an additional camera to ensure the stability of network geometry but it can avoid the complex experimental set-ups.

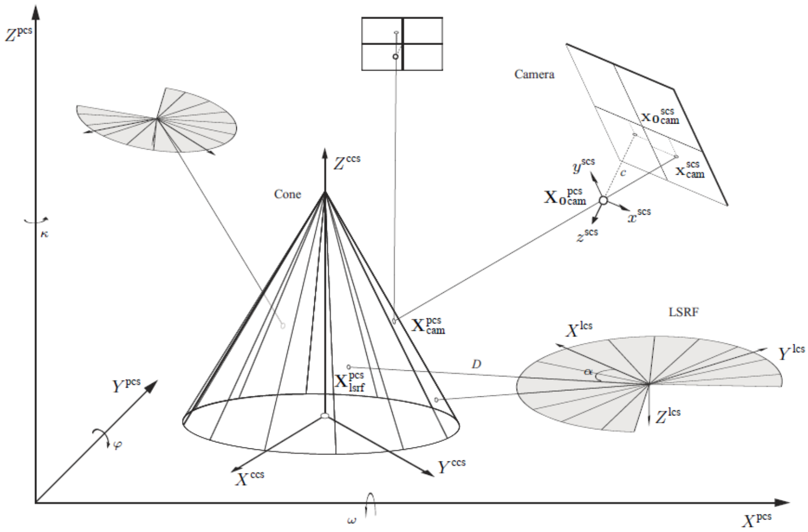

Figure 2- 7 Geometric model (Mader et al., 2014)

The above methods calibrate a single laser scanner, the 3D laser scanning system which comprises of 2D laser scanners can also be calibrated directly (Sheehan et al., 2012). Their set of calibration parameters for laser i is $\Theta_i = [\lambda_i, \tau_i, \alpha_i]^T$,λ is the distance of the beam origin from the center of the plate, τ is the angle between the laser scanning plane and the tangent vector to the plate, α is the angle between beam origins.

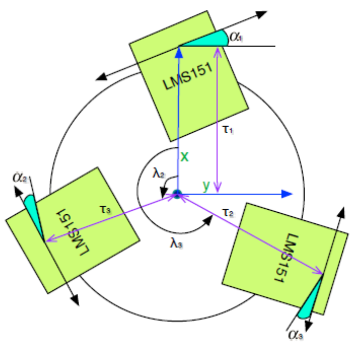

Figure 2- 8 Location of laser i on the plate (Sheehan et al., 2012)

Their calibration method has maxed the crispness of point cloud. They represent p(x) as Gaussian mixture model (GMM)

$$p(x) = \frac{1}{N}\sum_{i=1}^{N} G(x - \hat{x}_i, \sigma^2 I) \tag{2.7}$$

Where p(x) is the probability of drawing measurement from a given a location. $G(\mu, \sum)$ is the Gaussian with mean μ and covariance ∑, i is the measurement number. The 'crispness' of the point cloud can be linked to entropy of p(x), the more crisp the point cloud, the more peaky the distribution p(x) is.

They quantified the crispness of point cloud by a measure of entropy-RQE, and then they proposed the calibration model which only depends on the distances between two measured points.

$$E(\hat{X}) = -\sum_{i=1}^{N}\sum_{j=1}^{N} G(\hat{x}_i - \hat{x}_j, 2\sigma^2 I) \tag{2.8}$$

Where $\sigma^2 I$ is an isotropic kernel, i,j are measurement number, $\hat{x}_i - \hat{x}_j$ is the distance between two measured points.

They have investigated the accuracy of the calibration in both real and simulated data by treating the point cloud measurements as samples drawn from pdf covering the true underlying environment.

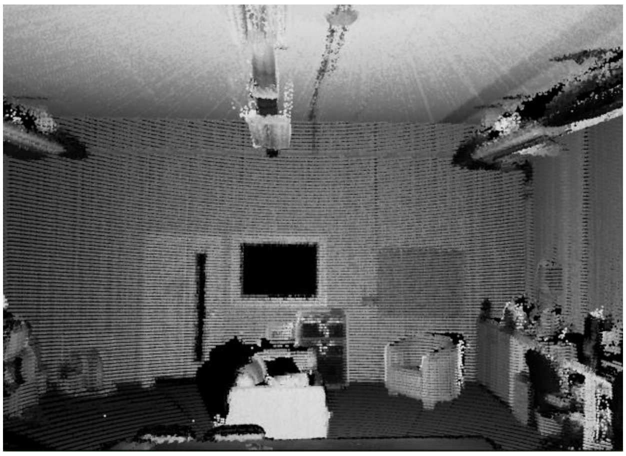

Figure 2- 9 An indoor environment created by the calibrated scanning system (Sheehan et al., 2012)

2.4 Summary

This chapter mainly introduced the 3 basic measuring principles of laser scanning technology, which are discrete pulse time of flight, phase measurements in continuous modulated waves and triangulation. Also, the main systems for indoor mapping have been introduced. At last, the calibration methods have reviewed by the calibration using references and self-calibration categories.

3 METHODOLOGY

In this chapter, the flow and method have been introduced. Section 3.1 describes the framework of the research. Section 3.2 describes how to collect data. Section 3.3 describes the mathematical model formulation. Section 3.4 describes how to analyze the noise after calibration.

3.1 Framework

There are 3 major steps in this process: data collection, formulation of mathematical model and accuracy analysis.

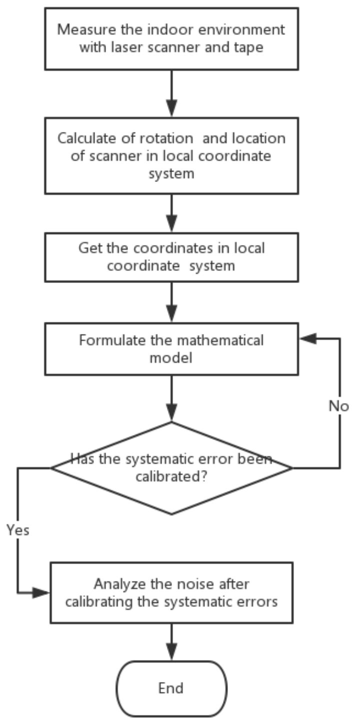

Figure 3- 1 Flowchart of the methodology

3.2 Data collection

3.2.1 Chosen indoor environment

The indoor environment for the research is classroom 2-010 of ITC building, Enschede, The Netherlands. The classroom is surrounded by white walls, which can lead to a more accurate acquired data because darker environment may absorb the emitted signals from the laser scanner. Also, the classroom is nearly a rectangle and size of the classroom is suitable for the research.

Figure 3- 2 Chosen indoor environment

Despite it looks a rectangle, this indoor environment isn't rectangular based on its plan, and there are obstacles at the corners of some walls, which makes only measuring the lengths of 4 walls less accurate, so a special measurement will be introduced in section 3.2.2.

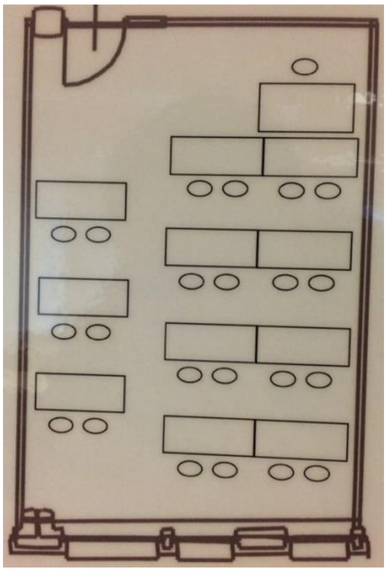

Figure 3- 3 Plan of the indoor environment

Figure 3- 4 Obstacles at corner in the indoor environment

3.2.2 Data sources

There are 2 data sources in this step:

1. From laser scanner: the laser scanner has been first put at the corner of the indoor environment because it is a 270° open angle scanner, which means it has still 90° cannot emit signal at, putting it at the corner allows it get larger variety of measured ranges and thereby better estimate the calibration parameters. In order to analyze the time effect, it scanned the walls for 20 minutes and recorded all the data. After the scanner cooled down, it has been put at the center of the indoor environment and recorded the data of 20 minutes, putting at the center of the classroom allows us to see whether there is effect when putting it at different location.
2. Reference data from the tape. Ideally, the lengths of walls should have also been directly measured by the tape. However, due to the non-rectangularity of the room and obstacles of corners, another method which indirectly measures the lengths of walls has been taken.

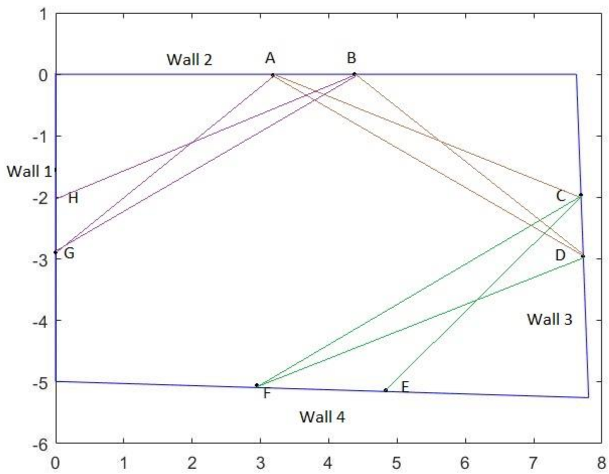

Figure 3- 5 Measurement of the indoor environment using tape

In this measurement, 2 points on each wall have been chosen at first, then the lengths of wall 2 and wall 3, the lengths of line AB,BD,AD,AC,CD; CD,DF,CF,CE,FE; HG,BG,HB,AG,AB have been measured.

With the lengths of above lines, the angles between walls can be calculated.

An example using AB,BD,AD,AC,CD to calculate the angles has been given below:

With the lengths of AB,AD,BD, using the law of cosine, angle BAD can be calculated, with the lengths of AC,AD,CD, angle ADC can be calculated. So the angle between wall 2 and wall 3 can be known as (180-∠BAD-∠ADC). The expression of wall 2 is y=0, the slope of wall 2 is 0, with the angle between wall 2 and wall 3, the slope of wall 3 can be calculated as 0+Angle.

The x coordinate of intersected point of wall 2 and wall 3 is the length of wall 2,and then the expression of wall 3 can be calculated

Applying the same principle, the expressions of other walls can be calculated and expressed in the form:

$$y = kx + b. \tag{3.1}$$

Normalize the coefficients of x and y, the expressions can be converted to the form

$$x * cos\theta + y * sin\theta - d = 0 \quad (3.2)$$

A locally 2D model coordinate system is defined here, whose X axis lies on wall 2 and origin point is the intersected point.

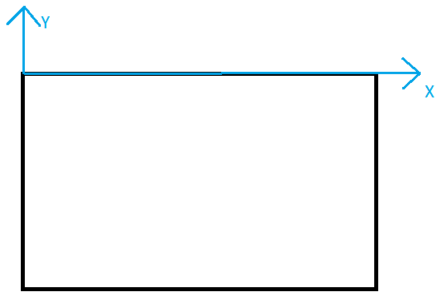

Figure 3- 6 Illustration of the locally defined coordinate system

3.3 Formulation of mathematical model

In this step, the measured points and reference data have been plotted, then the residual pattern has been inspected and the calibration parameters of scale and offset have been added one by one.

3.3.1 Calculation of rotation and location of the scanner

In the step of the formulation of mathematical model, the coordinates measured by laser scanner in the sensor coordinate system are already known in the step 3.2. Then the mathematical model can be formulated by those coordinates and the description of locations of walls (θ ,d) calculated in step 3.2.

The following equation describes relationship between coordinates in sensor coordinate system and locally defined model coordinate system, where X_m,Y_m are the coordinates in the locally defined model coordinate system, β is the rotation of the scanner, X_s and Y_s are the coordinates in the sensor coordinate system, X_0 and Y_0 are the location of scanner in locally defined coordinate system.

$$\begin{pmatrix} X_m \\ Y_m \end{pmatrix} = \begin{pmatrix} \cos\beta & \sin\beta \\ -\sin\beta & \cos\beta \end{pmatrix} \begin{pmatrix} X_s \\ Y_s \end{pmatrix} + \begin{pmatrix} X_0 \\ Y_0 \end{pmatrix} \quad (3.3)$$

The locations of walls can be described by the following equation where X_m,Y_m are the coordinates in the locally defined model coordinate system, θ and d are the parameters describing the location of wall .

$$X_m * \cos\theta + Y_m * \sin\theta - d = 0 \quad (3.4)$$

Replacing the X_m, Y_m in equation (3. 4) by the parameters of equations (3.3) can get

$$X_s * cos\beta * cos\theta + Y_s * sin\beta * cos\theta + X_0 * cos\theta - X_s * sin\beta * sin\theta + Y_s * cos\beta * sin\theta + Y_0 * sin\theta - d = 0 \quad (3.5)$$

The approximate values of β, X_0 and Y_0. can be estimated by looking at the plot of all the measured points. The approximate values are denoted as β^0,X_0^0,Y_0^0.

The increment to β, X_0 and Y_0 have been included to get the estimation. The estimation of increment of these parameters can be done by least squares. Then the equation 3.3 can be transformed into:

$$X_s(n) * cos(\beta^0) * cos(\theta) - \Delta\beta * X_s(n) * sin(\beta^0) * cos(\theta) + Y_s(n) * sin(\beta^0) * cos(\theta) + \Delta\beta * Y_s(n) * cos(\beta^0) * cos(\theta) + X_0^0 * cos(\theta) + \Delta X_0 * cos(\theta) - X_s(n) * sin(\beta^0) * sin(\theta) - \Delta\beta * X_s(n) * cos(\beta^0) * sin(\theta) + Y_s(n) * cos(\beta^0) * sin(\theta) - \Delta\beta * Y_s(n) * sin(\beta^0) * sin(\theta) + Y_0^0 *$$

$sin(\theta) + \Delta Y_0 * sin(\theta) - d = 0$ (3.6)

n is the observation number.

The coefficients for A and b of $A * x = b$, which is the calculation of increments based on the observations can be expressed as follows:

$$\begin{aligned} \mathrm{b(n)} = &-\mathrm{Xs\,(n)cos\,\theta\,cos\,\beta^0} \\ &- \mathrm{Ys\,(n)cos\,\theta\,sin\,\beta^0} \\ &- \mathrm{X0^0\,cos\,\theta + Xs\,(n)sin\,\theta\,sin\,\beta^0 - Ys\,(n)sin\,\theta\,cos\,\beta^0 - Y0^0\,sin\,\theta + d} \end{aligned}$$

$$A1(n) = -X_S\,(\mathrm{n})\cos\theta\sin\beta^0 + Y_S\,(\mathrm{n})\cos\theta\cos\beta^0 - X_S\,(\mathrm{n})\sin\theta\cos\beta^0 - Y_S\,(\mathrm{n})\sin\theta\sin\beta^0$$

$$\mathrm{A2(n) = \cos\theta}$$

$$\mathrm{A3(n) = \sin\theta}$$

$$\mathrm{A(n*3)} = \begin{bmatrix} \mathrm{A1(1)} & \mathrm{A2(1)} & \mathrm{A3(1)} \\ \mathrm{A1(2)} & \mathrm{A2(2)} & \mathrm{A3(2)} \\ \vdots & \vdots & \vdots \\ \mathrm{A1(n)} & \mathrm{A2(n)} & \mathrm{A3(n)} \end{bmatrix}$$

So the increments of the three parameters $x = \begin{bmatrix} \Delta\beta \\ \Delta X_0 \\ \Delta Y_0 \end{bmatrix}$ can be calculated as

$$x = (A^T A)^{-1} A^T b \tag{3.7}$$

Above equation is the least square estimation, which can give precise estimation of the increments.

With the accurate values for the rotation of the scanner (β) and the location of scanner in locally defined coordinate system (X_0 and Y_0), the coordinates of the measured points in locally defined coordinate system can be calculated and plotted. Compare the plot and with the data measured by tape, then the residuals can be seen and calculated. The residuals and RMS are calculated using:

$$\mathrm{e} = |x * cos\theta + y * sin\theta - d| \tag{3.8}$$

$$\mathrm{RMS} = \sqrt{\mathrm{e}^2/\mathrm{n}} \tag{3.9}$$

Also, the plot of the average remaining residuals as a function of the range has also been drawn to understand the errors better.

Iterate the above process until there are no changes for β, X_0 and Y_0.

Then the plots and RMS have been analyzed to see if there are parameters to add to calibrate the measured range.

3.3.2 Calculation of added parameter scale

The pattern of the residuals can be inspected after analyzing the plots. Then the scale parameter has been added to the measured range to calibrate the scanner. Due to the original data is the coordinates in the sensor coordinate system, the range r and scanning direction α have been calculated using following equations:

$$r = \sqrt{X_S{}^2 + Y_S{}^2} \tag{3.10}$$

$$\alpha = \arctan\left(\frac{Y_S}{X_S}\right) \tag{3.11}$$

Because
$$\begin{pmatrix} X_S \\ Y_S \end{pmatrix} = \begin{pmatrix} \cos\alpha & \sin\alpha \\ -\sin\alpha & \cos\alpha \end{pmatrix} \begin{pmatrix} r \\ 0 \end{pmatrix} \quad (3.12)$$

The equation (3.3) can be expressed as below:

$$(r\cos\alpha\cos\beta - r\sin\alpha\sin\beta + X_0)\cdot\cos\theta + (-r\cos\alpha\sin\beta - r\sin\alpha\cos\beta + Y_0)\cdot\sin\theta - d = 0 \quad (3.13)$$

Replacing range r with the newly added parameter scale k

$$\hat{r} = k * r \quad (3.14)$$

The coordinates in sensor coordinate system based on the observed range r and scanning direction α can be calculated as below, where X_s and Y_s are the coordinates in the sensor coordinate system.

$$\begin{pmatrix} \widehat{X_S} \\ \widehat{Y_S} \end{pmatrix} = \begin{pmatrix} \cos\alpha & \sin\alpha \\ -\sin\alpha & \cos\alpha \end{pmatrix} \begin{pmatrix} \hat{r} \\ 0 \end{pmatrix} \quad (3.15)$$

In equation (3.13), the values for the rotation of the scanner (β) and the location of scanner in locally defined coordinate system (X_0 and Y_0) can be known from step 3.3.1. After linearizing the three parameters and added parameter scale, again using least squares can get the estimation of increment of these parameters.

The equation (3.9) can be transformed into:

$$k^0 * r(n) * cos(\alpha) * cos(\theta) * cos(\beta^0) + \triangle k * r(n) * cos(\alpha) * cos(\theta) * cos(\beta^0) - \triangle \beta * k^0 * r(n) * cos(\alpha) * cos(\theta) * sin(\beta^0) - k^0 * r(n) * sin(\alpha) * cos(\theta) * sin(\beta^0) - \triangle k * r(n) * sin(\alpha) * cos(\theta) * sin(\beta^0) - \triangle \beta * k^0 * r(n) * sin(\alpha) * cos(\theta) * cos(\beta^0) + X0^0 * cos(\theta) + \triangle X0 * cos(\theta) - k * r(n) * cos(\alpha) * sin(\theta) * sin(\beta^0) - \triangle k * r(n) * cos(\alpha) * sin(\theta) * sin(\beta^0) - \triangle \beta * k^0 * r(n) * cos(\alpha) * sin(\theta) * cos(\beta^0) - k0 * r(n) * sin(\alpha) * sin(\theta) * cos(\beta^0) - \triangle k * r(n) * sin(\alpha) * sin(\theta) * cos(\beta^0) + \triangle \beta * k^0 * r(n) * sin(\alpha) * sin(\theta) * sin(\beta^0) + Y0^0 * sin(\theta) + \triangle Y0 * sin(\theta) - d = 0 \quad (3.16)$$

n is the observation number.

The coefficients of $AX = b$, which is the calculation of increments of the 4 parameters can be expressed as follows:

$$b(n) = -(k^0 * r(n) * cos(\alpha) * cos(\theta) * cos(\beta^0) - k^0 * r(n) * sin(\alpha) * cos(\theta) * sin(\beta^0) + X_0{}^0 * cos(\theta) - k^0 * r(n) * cos(\alpha) * sin(\theta) * sin(\beta^0) - k^0 * r(n) * sin(\alpha) * sin(\theta) * cos(\beta^0) + Y_0{}^0 * sin(\theta) - d)$$

$$A1(n) = r(n) * cos(\alpha) * cos(\theta) * cos(\beta^0) - r(n) * sin(\alpha) * cos(\theta) * sin(\beta^0) - r(n) * cos(\alpha) * sin(\theta) * sin(\beta^0) - r(n) * sin(\alpha) * sin(\theta) * cos(\beta^0)$$

$$A2(n) = -k * r * cos(\alpha) * cos(\theta) * sin(\beta) - k * r * sin(\alpha) * cos(\theta) * cos(\beta) - k * r * cos(\alpha) * sin(\theta) * cos(\beta) + k * r * sin(\alpha) * sin(\theta) * sin(\beta)$$

$$A3(n) = cos(\theta)$$

$$A4(n) = sin(\theta)$$

$$A(n*4) = \begin{bmatrix} A1(1) & A2(1) & A3(1) & A4(1) \\ A1(2) & A2(2) & A3(2) & A4(2) \\ \vdots & \vdots & \vdots & \vdots \\ A1(n) & A2(n) & A3(n) & A4(n) \end{bmatrix}$$

n is the observation number.

So the increments for the 4 parameters $x=\begin{bmatrix}\Delta k\\ \Delta \beta\\ \Delta X_0\\ \Delta Y_0\end{bmatrix}$ can be calculated using equation (3.7)

Like I step 3.3.2, the least square estimation gives the precise estimation of the increments to the 4 parameters.

Then use equation (3.3) to calculate the coordinates in model coordinate system and plot the calibrated coordinates and compare it with the walls measured by tape and calculate the residuals and RMS by (3.8), (3.9). After that, the plot of the average remaining residuals as a function of the range has also been drawn.

Iterate the 3.3.2 until there are no changes for k, β, X_0 and Y_0.

The plots and RMS then have been analyzed to see if there are other addable parameters to calibrate the scanner.

3.3.3 Calculation of added parameter offset

The offset parameter i has been added to the range to calibrate the measurement after analyzing the residuals.

So the accurate range r can be expressed as:

$$\hat{r} = (k^0 + \Delta k) * r + i + \Delta i \tag{3.17}$$

So the coordinate in the sensor coordinate system can be calculated as:

$$\begin{pmatrix} X_S \\ Y_S \end{pmatrix} = \begin{pmatrix} \cos\alpha & \sin\alpha \\ -\sin\alpha & \cos\alpha \end{pmatrix} \begin{pmatrix} \hat{r} \\ 0 \end{pmatrix} \tag{3.18}$$

After linearizing the three parameters and added parameters scale k and offset to range i, again using least squares can get the estimation of increment of these parameters.

The equation (3.13) can be transformed into:

$$k^0 * r(n) * cos(\alpha) * cos(\beta^0) * cos(\theta) - \Delta \beta * k^0 * r(n) * cos(\alpha) * sin(\beta^0) * cos(\theta) + \Delta k * r(n) * cos(\alpha) * cos(\beta^0) * sin(\theta) + \Delta i * cos(\alpha) * cos(\beta^0) * cos(\theta) - k^0 * r(n) * sin(\alpha) * sin(\beta^0) * cos(\theta) - k^0 * \Delta \beta * r(n) * sin(\alpha) * cos(\beta^0) * cos(\theta) - \Delta k * r(n) * sin(\alpha) * sin(\beta^0) * cos(\theta) - \Delta i * sin(\alpha) * sin(\beta^0) * cos(\theta) + X0^0 * cos(\theta) + \Delta X0 + cos(\theta) - k^0 * r(n) * cos(\alpha) * sin(\beta^0) * sin(\theta) - \Delta \beta * k^0 * r(n) * cos(\alpha) * cos(\beta^0) * sin(\theta) - \Delta k * r(n) * cos(\alpha) * sin(\beta^0) * sin(\theta) - \Delta i * cos(\alpha) * sin(\beta^0) * sin(\theta) - k^0 * r(n) * sin(\alpha) * cos(\beta^0) * sin(\theta) + \Delta \beta * k^0 * r(n) * sin(\alpha) * sin(\beta^0) * sin(\theta) - \Delta k * r(n) * sin(\alpha) * cos(\beta^0) * sin(\theta) - \Delta i * sin(\alpha) * cos(\beta^0) * sin(\theta) + Y0^0 * sin(\theta) + \Delta Y0 * sin(\theta) + i^0 * cos(\alpha) * cos(\beta^0) * cos(\theta) - \Delta \beta * i^0 * cos(\alpha) * sin(\beta^0) * cos(\theta) - i^0 * sin(\alpha) * sin(\beta^0) * cos(\theta) - \Delta \beta * i^0 * sin(\alpha) * cos(\beta^0) * cos(\theta) - i^0 * cos(\alpha) * sin(\beta^0) * sin(\theta) - \Delta \beta * i^0 * cos(\alpha) * cos(\beta^0) * sin(\theta) - i^0 * sin(\alpha) * cos(\beta^0) * sin(\theta) + \Delta \beta * i^0 * sin(\alpha) * sin(\beta^0) * sin(\theta) - d = 0 \tag{3.19}$$

n is the observation number.

The coefficients of $AX = b$, the calculation of the increments of 5 parameters based on the observations can be expressed as follows:

$$b(n) = -(k^0 * r(n) * cos(\alpha) * cos(\beta^0) * cos(\theta) - k^0 * r(n) * sin(\alpha) * sin(\beta^0) * cos(\theta) + {X_0}^0 * cos(\theta) - k^0 * r(n) * cos(\alpha) * sin(\beta^0) * sin(\theta) - k^0 * r(n) * sin(\alpha) * cos(\beta^0) * sin(\theta) + {Y_0}^0 * sin(\theta) - d)$$

$$A1(n) = cos(\alpha) * cos(\beta^0) * cos(\theta) - sin(\alpha) * sin(\beta^0) * cos(\theta) - cos(\alpha) * sin(\beta^0) * sin(\theta) - sin(\alpha) * cos(\beta^0) * sin(\theta)$$

$$A2(n) = r(n) * cos(\alpha) * cos(\beta^0) * cos(\theta) - r(n) * sin(\alpha) * sin(\beta^0) * cos(\theta) - r(n) * cos(\alpha) * sin(\beta^0) * sin(\theta) - r(n) * sin(\alpha) * cos(\beta^0) * sin(\theta)$$

$$A3(n) = -k^0 * r(n) * cos(\alpha) * sin(\beta^0) * cos(\theta) - k^0 * r(n) * sin(\alpha) * cos(\beta^0) * cos(\theta) - k^0 * r(n) * cos(\alpha) * cos(\beta^0) * sin(\theta) + k^0 * r(n) * sin(\alpha) * sin(\beta^0) * sin(\theta) - i^0 * cos(\alpha) * sin(\beta^0) * cos(\theta) - i^0 * sin(\alpha) * cos(\beta^0) * cos(\theta) - i^0 * cos(\alpha) * cos(\beta^0) * sin(\theta) + i^0 * sin(\alpha) * sin(\beta^0) * sin(\theta)$$

$$A4(n) = cos(\theta)$$

$$A5(n) = sin(\theta)$$

$$\mathrm{A}(\mathrm{n} * 5) = \begin{bmatrix} \mathrm{A1(1)} & \mathrm{A2(1)} & \mathrm{A3(1)} & \mathrm{A4(1)} & \mathrm{A5(1)} \\ \mathrm{A1(2)} & \mathrm{A2(2)} & \mathrm{A3(2)} & \mathrm{A4(2)} & \mathrm{A5(2)} \\ \vdots & \vdots & \vdots & \vdots & \vdots \\ \mathrm{A1(n)} & \mathrm{A2(n)} & \mathrm{A3(n)} & \mathrm{A4}(n) & \mathrm{A5}(n) \end{bmatrix}$$

n is the observation number.

So the increments of the 5 parameters x= $\begin{bmatrix} \Delta i \\ \Delta k \\ \Delta \beta \\ \Delta X0 \\ \Delta Y0 \end{bmatrix}$ can be calculated using equation (3.7)

Then use equation (3.3) to calculate the coordinates in model coordinate system and plot the calibrated coordinates and compare it with the walls measured by tape and calculate the residuals and RMS by (3.8), (3.9). After that, the plot of the average remaining residuals as a function of the range has also been drawn.

Iterate the 3.3.3 until there are no changes for i, k, β, X_0 and Y_0.

Then the plots and RMS have been analyzed.

3.3.4 More parameters

The residual between the measured points and reference data has been enlarged 10 times to see if there still is systematic error.

3.4 Noise analysis

This step is to analyze how accurate the scanner can be after calibration. The random errors when using this laser scanner have been studied; mainly focus on the accuracy change over range and time.

3.4.1 Accuracy over range

Accuracy over range has been analyzed by comparing the random errors of different ranges at interval of 0.5m, the plots of standard deviation and mean absolute value of noise on range with range in certain intervals have been drawn in order to understand the accuracy after calibrating the laser scanner.

3.4.2 Accuracy over time

There are 2 main aspects in this part.

First aspect is warm-up problem and overheating problem. The data has been collected since the beginning to the 20th minute. I chose the data with 5 minutes interval to see where the largest change in RMS is, then I can see if there is large change in RMS in all the minutes in that interval. The stability of RMS values and parameters is used to evaluate the accuracy of the scanner.

Second aspect is to analyze if we need to recalibrate the laser scanner after a longer time not using it, e.g. 1 week. The RMS value and the values of added parameters are used to compare the accuracy between the datasets acquired with a longer time gap.

4 IMPLEMENTATION AND ANALYSIS

This chapter first introduces the basic information of the laser scanner needs calibrating. Then the results of the pre-process of data and major steps of the calibration of the scanner have been given. The accuracy of the calibrated scanner has then been evaluated. These steps are implemented in Point Cloud Mapper (PCM) and Matlab R2015b.

Section 4.1 introduces the specification of the laser scanner. Section 4.2 describes the pre-process of data. From section 4.3 to section 4.7 describes the results of major steps in the calibration. Section 4.8 analyzes the accuracy of the laser scanner after calibration.

4.1 Specification of scanner

The scanner we calibrate is Hokuyo UTM-30LX, which uses laser source with λ=905nm to measure the distance to objects in the range with 270°open angle. It stores the coordinates of the points calculated using the step angle, the measurement along with angle are transmitted by communication channel. It can guarantee its accuracy which is 3cm under 3000lx and 5 cm under 1000000 lx for white kent sheet in the range of 0.1-30m and its maximum range is 60m. It is capable of detecting the object in width from 130mm to 10m (Hokuyo Ltd, 2012).

Figure 4- 1 Hokuyo UTM-30LX (Hokuyo Ltd, 2012)

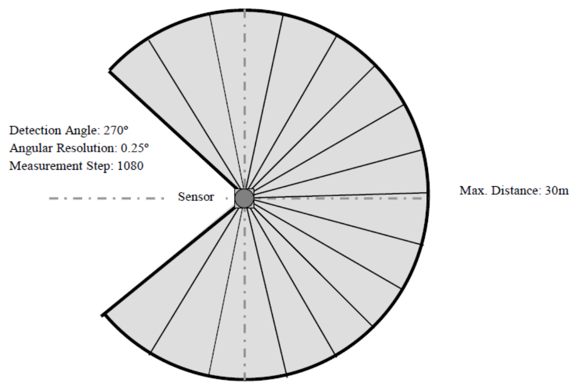

Figure 4- 2 Structure of the laser scanner (Hokuyo Ltd, 2012)

4.2 Pre-process data

4.2.1 Reference data

The reference data is acquired using the method mentioned in 3.3.2. Each length is measured twice to verify its accuracy. In order to show the accuracy of measurement, I here listed the original measured lengths dividing into 3 sets of data with lengths corresponds to figure 3-5.

Table 4- 1 Measured lengths in the triangle ACD, ABD

	AD	BD	AB	AC	CD
1^{st} (m)	7.295	4.360	5.010	5.878	3.010
2^{nd} (m)	7.297	4.358	5.008	5.880	3.009
Difference(m)	-0.002	0.002	0.002	-0.002	0.001

Table 4- 2 Measured lengths in the triangle CDF, CEF

	CF	DF	CD	CE	FE
1^{st}(m)	7.835	6.982	3.010	4.065	6.013
2^{nd}(m)	7.834	6.982	3.009	4.066	6.013
Difference(m)	0.001	0.000	0.001	-0.001	0.000

Table 4- 3 Measured lengths in the triangle BGH, ABG

	BG	BH	HG	AG	AB
1^{st}(m)	7.923	7.090	2.483	4.240	5.010
2^{nd}(m)	7.922	7.092	2.485	4.240	5.008
Difference(m)	0.001	-0.002	-0.002	0.000	0.002

Table 4- 4 Measured lengths of wall 2 and wall 3

	Wall 2	Wall 3
1^{st} (m)	7.635	5.265
2^{nd} (m)	7.635	5.267
Difference(m)	0.000	-0.002

From the tables above, we can see there is only very little difference in the 2 measurements, which means the measurements are very accurate. I then took the average value of 2 measurements as the length, after calculation using method mentioned in 3.3.2, the final lengths of walls are:

Table 4- 5 Lengths of each wall in the classroom

	Wall 1	Wall 2	Wall 3	Wall 4
Length (m)	5.2676	7.6350	5.2660	7.9463

4.2.2 Laser data

The laser data have been acquired at 2 locations, first one is at the corner of the classroom, and second is at the center of the classroom. The scanner recorded data for 20 minutes at each location. In order to identify the number of datasets, I used first number to label at which minute the data was acquired. The number after the hyphen indicates in which scanline the data acquired. E.g. dataset 1-2 means the data acquired at 1st minute at 2nd scanline.

The original laser data acquired is in the format of number of point, measured distance, beam intensity and time. The coordinates in the sensor coordinate system has been then calculated by range and angle.

The coordinates in the sensor coordinate system then can be seen in PCM, the points have been manually labeled with their corresponding wall index. For each scanline, the points are labeled like this but slightly different because this is pure manual process. The non-labeled points at the center are the chairs and tables. The non-labeled points close to the walls are obstacles which can only be seen in reality.

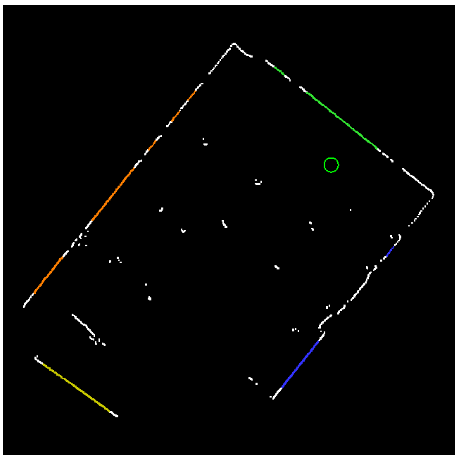

Figure 4- 3 Labeling the measured points with corresponding walls

Using method mentioned in chapter 3, the coordinates in model coordinate system and RMS value can be calculated in further steps.

4.3 Convergence

For all the datasets, the rotation of scanner (β), location of scanner in the model coordinate system (X_0,Y_0) converge after each step. An example is given using data 2-1 of the data acquired at the corner of classroom and data 5-1 of the data acquired at the center of the classroom.

The first column is the estimated values for β, X_0 and Y_0 by looking at the difference of plot of the coordinates in the sensor coordinate system and the model coordinate system. The 1st step refers to section 3.3.1 calculation of rotation and location of the scanner, 2nd step is section 3.3.2 calculation of parameter scale and 3rd step is 3.3.3 calculation of parameter offset.

The iteration will stop when the values for the three parameters don't change anymore. I only chose 2 digits after decimal point for β and 4 digits after decimal point for X_0 and Y_0 in tables below.

Table 4- 6 Values for β, X0 and Y0 in the data 2-1 of the data acquired at the corner

	1st step			2nd step	3rd step
Iteration number	1	2	3-8	1-4	1-8
β(°)	-130.00	-128.83	-128.79	-128.91	-128.94
X_0(m)	7.0000	6.5756	6.5766	6.5686	6.5784
Y_0(m)	-1.0000	-1.0618	-1.0629	-1.0625	-1.0532

The values for all the three parameters came very close since 3rd iteration in the first step, we cannot see the difference because I only show 4 digitals after decimal point. The values also came close at 2nd and 3rd step.

Table 4- 7 Values for β, X0 and Y0 in the data 5-1 of the data acquired at the center

	1st step			2nd step	3rd step
Iteration number	1	2	3-7	1-5	1-8
β(°)	130.00	-128.68	-128.68	-128.72	-128.65
X_0(m)	5.5000	5.2641	5.2648	5.2576	5.2677
Y_0(m)	-4.0000	-2.0182	-2.0191	-2.0233	-2.0202

From the tables above, we can see that the values for the three parameters came to very close after the iterations in each step. At the first iteration, the program corrected more because the values at the first columns are the approximate values. We can conclude that the rotation of scanner (β), location of scanner in the model coordinate system (X_0,Y_0) converge well after all the steps.

4.4 Plots

The plots show the calibrated data has matched the reference data. The example is still given using data 2-1 of the data acquired at the corner of classroom and data 5-1 of the data acquired at the center of the classroom. I listed the plot of measured points and reference data after each step.

4.4.1 Data 2-1 of the data acquired at the corner of classroom

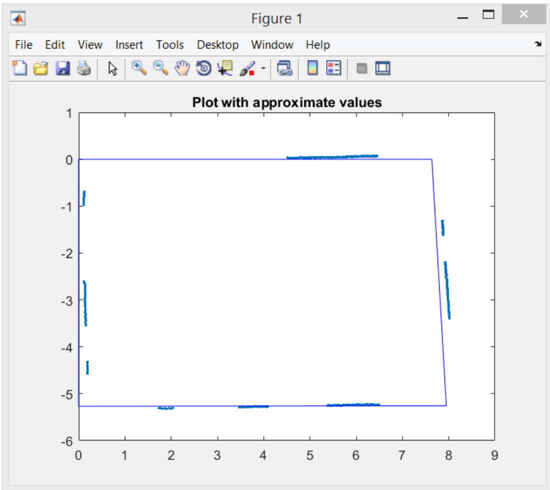

Figure 4- 4 Plot with the approximate values

Figure above is the measured points with approximate values for β,X_0,Y_0 and reference data. Clearly the measured points don't match the reference data.

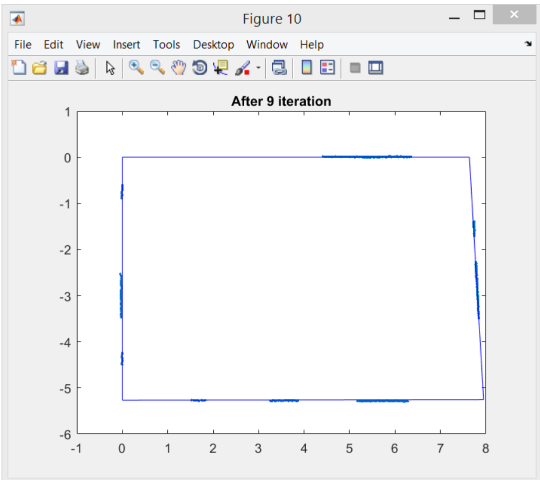

Figure 4- 5 Plot after 1st step

There is a systematic error judging by the figure above, the residuals on range have been enlarged 10 times on the direction the scanner beams to see the systematic error more clearly.

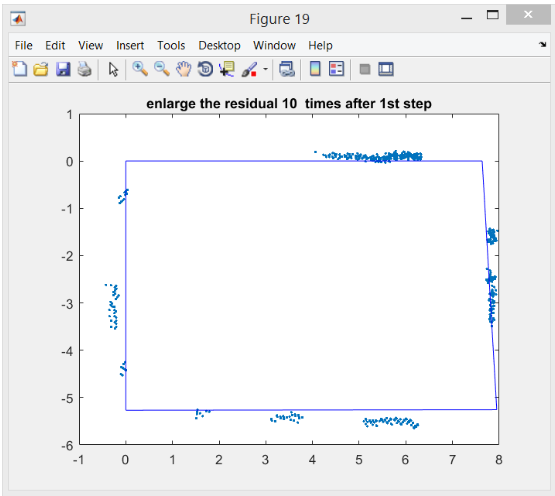

Figure 4- 6 Enlargement of residuals after 1st step

This shows that the measured points have matched the reference data better, however, the measured points are outward than reference data. So a scale factor has been included at next step.

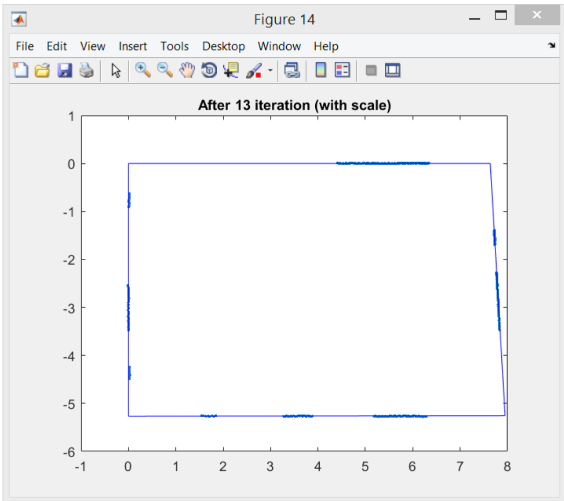

Figure 4- 7 Plot after 2nd step

The residuals have been enlarged 10 times to see if there is systematic error.

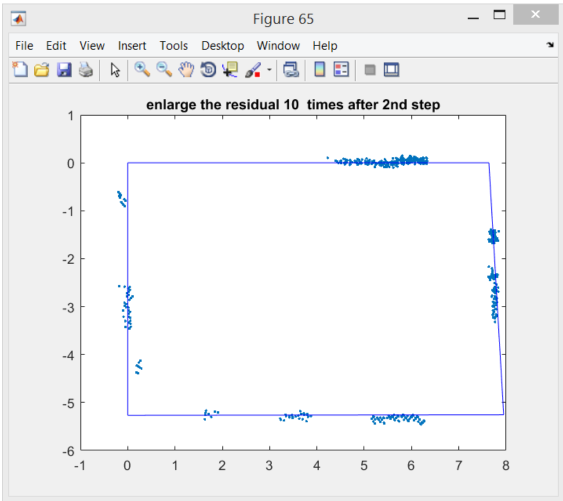

Figure 4- 8 Enlargement of residuals after 2nd step

The scale factor has made measured points matched the reference data better, in the next step, an offset parameter has been included.

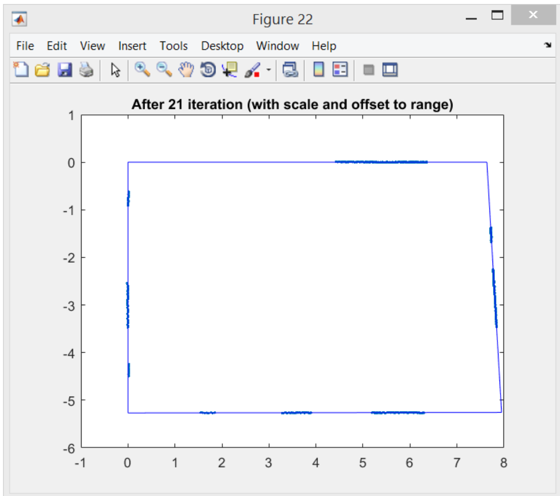

Figure 4- 9 Plot after 3rd step

The measured points have matched the reference better. To see if there are other calibration parameters to add to calibrate the scanner better, the residuals on range have been enlarged 10 times, so the pattern can be seen if there are still systematic errors.

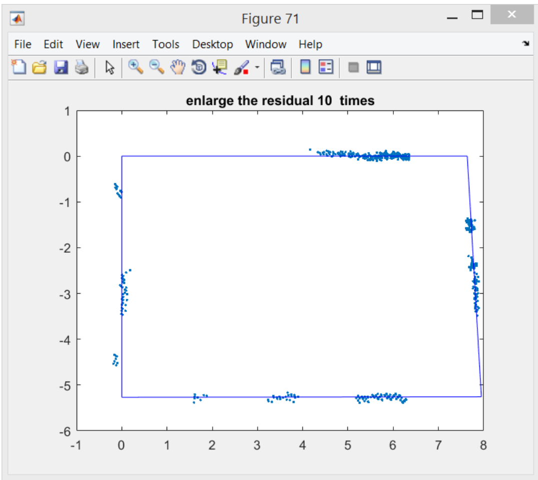

Figure 4- 10 Enlargement of residual 10 times for data 2-1 of the corner of classroom

There is no clear pattern of systematic error from above figure.
So we can see the clear systematic errors have been eliminated.

4.4.2 Data 5-1 of the data acquired at the center of classroom

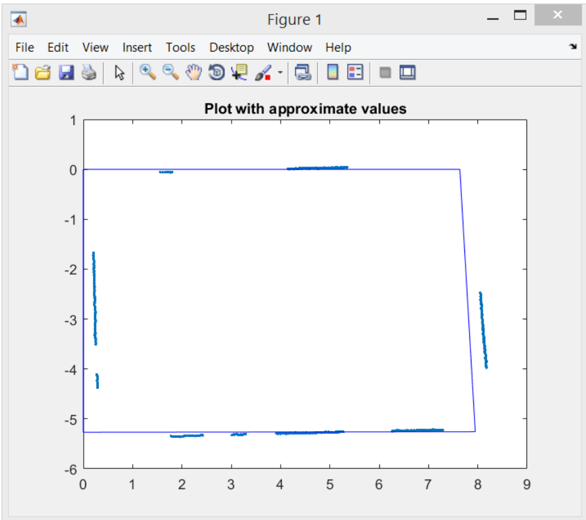

Figure 4- 11 Plot with approximate values

Figure above is the measured points with approximate values for β,X_0,Y_0 and reference data. Clearly the measured points don't match the reference data.

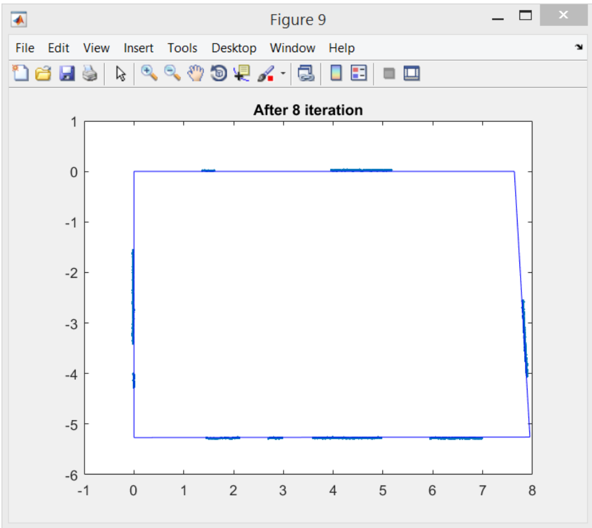

Figure 4- 12 Plot after 1st step

There is a systematic error judging by the figure above, the residuals on range have been enlarged 10 times on the direction the scanner beams to see the systematic error more clearly.

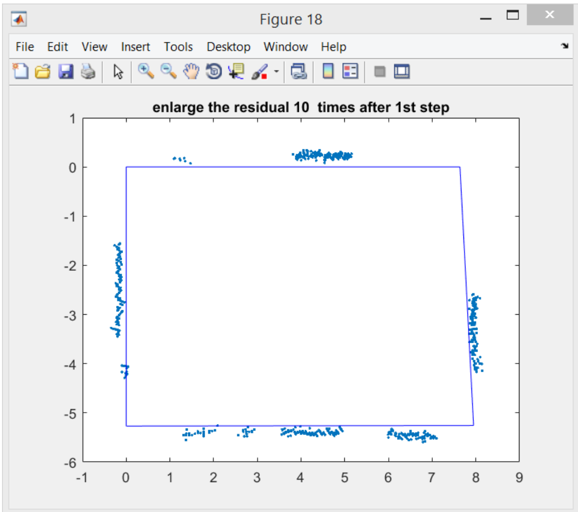

Figure 4- 13 Enlargement of residuals after 1st step

This shows that the measured points have matched the reference data better, however, the measured points are outward than reference data. So a scale factor has been included at next step.

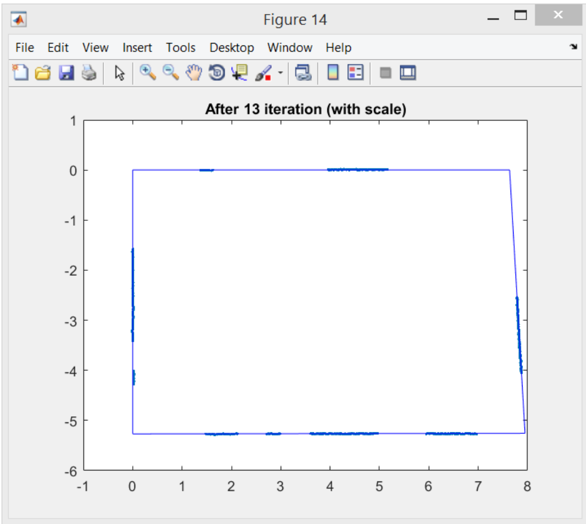

Figure 4- 14 Plot after 2nd step

The residuals have been enlarged 10 times to see if there is systematic error.

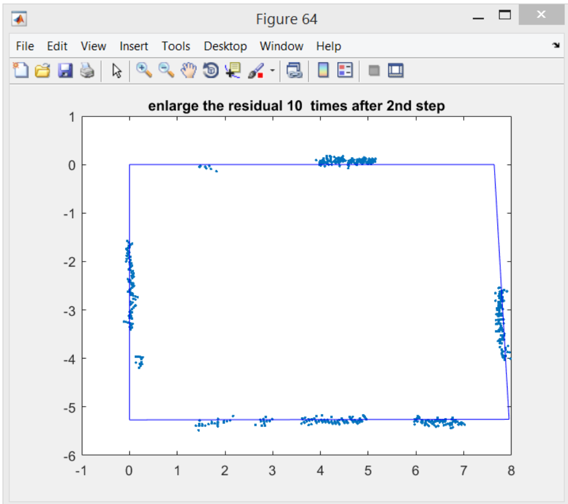

Figure 4- 15 Enlargement of residuals after 2nd step

The scale factor has made measured points matched the reference data better, in the next step, an offset parameter has been included.

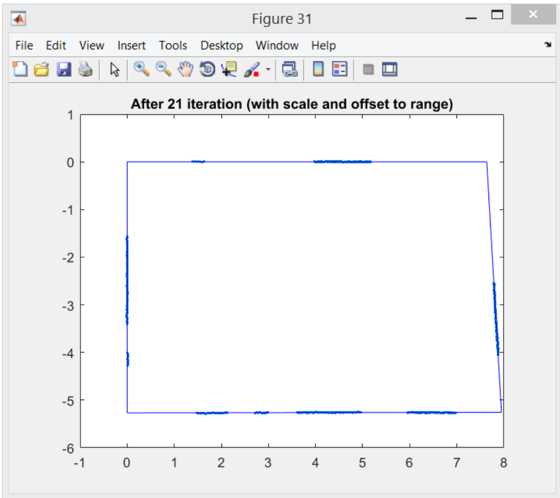

Figure 4- 16 Plot after 3rd step

The measured points have matched the reference better. But still to see if there is other calibration parameters can be added, the residuals have been enlarged 10 times on the direction scanner beams.

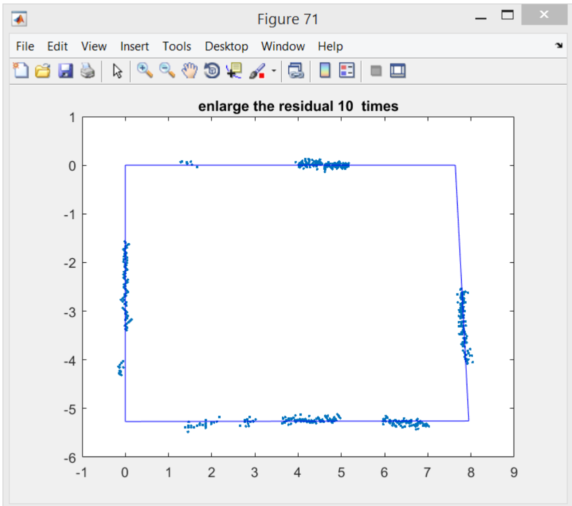

Figure 4- 17 Enlargement of residual 10 times for data 5-1 of the center of classroom

For the above figure, the pattern resembles a pincushion distortion as known for a lens distortion (Doxygen, 2015). But given the fact that the accuracy of calibrated scanner (0.7cm) is way below the guaranteed accuracy of the specification of the laser scanner 3cm, we can conclude that the scanner has been well calibrated.

We can conclude from plots of both datasets that the measured points have been clearly better matched the reference data after each step. This shows that calibration has improved the accuracy of the laser scanner.

4.5 RMS

In order to see how accurate the measured points is comparing with the reference data, here the RMS and RMS on range are used to evaluate the accuracy.

The RMS is calculated using equation (3.8), (3.9).

The RMS on range is to evaluate how accurate the scanner is at the direction it beams. It is calculated in 2 steps: step 1 is to calculate the intersected point (u,v) between the line (X_m,Y_m) (X_0,Y_0) and wall. Step 2 using the distance between (X_0,Y_0) and wall, i.e. line1, distance between (u,v) and (X_0,Y_0), i.e. line 2 and distance between (X_m,Y_m) and wall. The residuals on the range can be calculated. Again using $\mathrm{RMS} = \sqrt{e2/n}$, the RMS on range can be calculated. The residual on range is explained using figure 4-18.

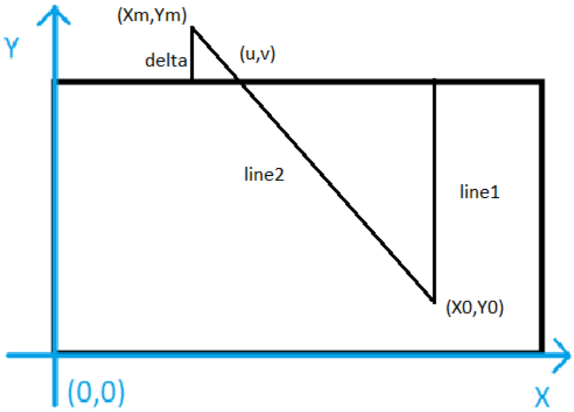

Figure 4- 18 Illustration of calculation of the RMS on range

The example is given using data 2-1 of the data acquired at the corner of classroom and data 5-1 of the data acquired at the center of the classroom.

Table 4- 8 Values of RMS and added parameters of data 2-1 of the corner of classroom

	1st step	2nd step	3rd step
RMS (m)	0.0148	0.0075	0.0059
RMS on range (m)	0.0172	0.0097	0.0077
k		0.9955	1.0011
i			-0.0218

Table 4- 9 Values of RMS and added parameters of data 5-1 of the center of classroom

	1st step	2nd step	3rd step
RMS (m)	0.0180	0.0078	0.0060
RMS on range (m)	0.0198	0.0088	0.0069
k		0.9948	1.0027
i			-0.0276

From the tables above we can conclude that the accuracy has been improved because both values of RMS and RMS on range have decreased. The RMS values are below the guaranteed accuracy 3 cm mentioned in the specification of the scanner.

The reason for the value of RMS on range is higher than its corresponding RMS value is that residual on range is the longer line in the triangle formed by the residual and residual on range, i.e. the length between (X_m,Y_m) and (u,v) is longer than delta in figure 4-18 .

4.6 Proposed calibration model

A calibration model has been proposed in this research, which is $\hat{r} = k * r + i$, where k is the scale factor and i is the offset for the range. In here, I chose 7 datasets in dataset acquired at the corner and 7 datasets acquired at the center to show the values of scale parameter and offset parameter.

Table 4- 10 Values for parameters of calibration model of data acquired at the corner

	1-1	2-1	5-1	10-1	15-1	20-1	20-2500
k	1.0013	1.0011	1.0018	1.0020	1.0008	1.0015	1.0010
i	-0.0243	-0.0218	-0.0255	-0.0256	-0.0202	-0.0230	-0.0229

Table 4- 11 Values for parameters of calibration model of data acquired at the center

	1-1	2-1	5-1	10-1	15-1	20-1	20-2500
k	1.0016	1.0021	1.0027	1.0026	1.0030	1.0022	1.0035
i	-0.0253	-0.0269	-0.0276	-0.0271	-0.0286	-0.0268	-0.0308

In order to see the accuracy of scale parameter k and offset parameter i, the theoretical accuracy has also been investigated.

The increment has been calculated using equation (3.7) $x = (A^T A)^{-1} A^T b$

So according to error propagation, the covariance matrix can be calculated as:

$$\sum x = (A^T A)^{-1} A^T \sigma^2 I A (A^T A)^{-1T} \tag{4.1}$$

I is identity matrix, A and b are the coefficients of the least square calculation, σ is the accuracy of the value of RMS on range.

In equation (4.1), the multiplication of $(A^T A)^{-1} A^T$ and the part IA is I, the transpose of $(A^T A)^{-1}$ is still $(A^T A)^{-1}$.

So equation (4.1) can be expressed as:

$$\sigma_x{}^2 = \sigma^2 (A^T A)^{-1} \tag{4.2}$$

Because the calculated parameters are in the sequence of $\begin{bmatrix} \Delta i \\ \Delta k \\ \Delta \beta \\ \Delta X0 \\ \Delta Y0 \end{bmatrix}$, so the covariance matrix is in the form:

$$\sigma_x{}^2 = \begin{bmatrix} \sigma_i{}^2 & & & & \\ & \sigma_k{}^2 & & & \\ & & \sigma_\beta{}^2 & & \\ & & & \sigma_{X0}{}^2 & \\ & & & & \sigma_{Y0}{}^2 \end{bmatrix}$$

The values of scale parameter k and offset parameter i are in the (1,1) and (2,2) in the above equation.

Table 4- 12 Mean and standard deviation of scale k and offset i of data acquired at the corner

	Mean value	Standard deviation	Theoretical accuracy
k	1.0013	0.0004	0.00045
i	-0.0233	0.0019	0.0017

Table 4- 13 Mean and standard deviation of scale k and offset i of data acquired at the center

	Mean value	Standard deviation	Theoretical accuracy
k	1.0025	0.0006	0.00049
i	-0.0275	0.0017	0.0017

We can see that the standard deviation (0.0004) of parameter scale k of data acquired at corner is lower than the standard deviation (0.0006) of parameter scale k of data acquired at the center of the classroom. This is because for the data acquired at the corner, it has a larger range of measured range. So the standard deviation of calculated parameter scale k, which is the slope of the proposed calibration model, is lower.

The scale factor is around 1.0020 and offset factor is around -0.0255. The reason for having different values in the parameters is that despite I tried to choose the points at the same location for each dataset, they cannot be exact the same points in each dataset.

The standard deviations of both scale parameter k and offset parameter i are near to the theoretical accuracy despite the scale factor of data acquired at the center is a little bit higher. Another thing to notice is that the mean value of scale k plus three times standard deviation is the mean value of the scale parameter k of data acquired at the center, which shows the difference between 2 values of scale factor can be significant, but this is due to labeling the points is a pure manual process.

4.7 Noise analysis after calibration

The noise analysis after the calibration procedure contains 2 parts: analysis of the accuracy over the measured range and accuracy over time.

4.7.1 Accuracy over range

The plots of absolute mean and standard deviation residual on range with the 0.5 m interval are shown to see the random errors. This step is to see in which range there is larger error. Still, the example is given using 3 datasets acquired at the corner of classroom and data 3 datasets acquired at the center of the classroom.

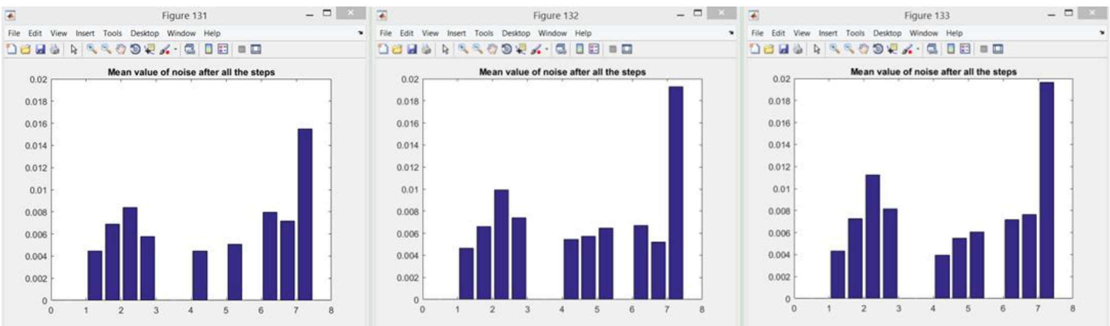

Figure 4- 19 Mean absolute values of residuals on range for data 2-1, 5-1, 10-1 of the corner of classroom

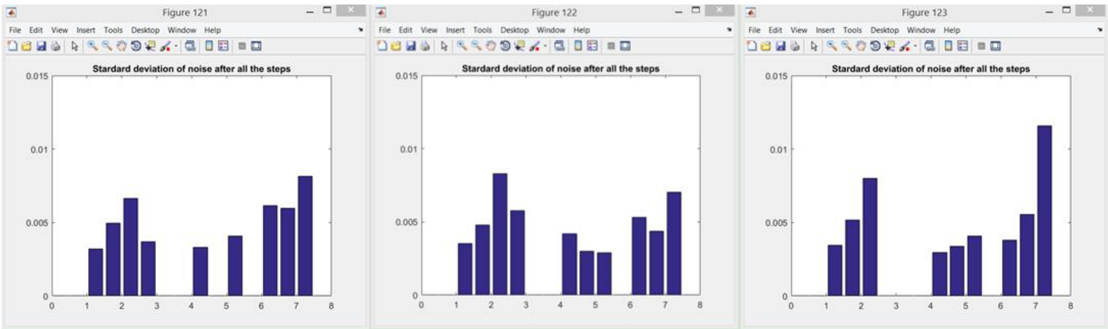

Figure 4- 20 Standard deviation of residuals on range for data 2-1, 5-1, 10-1 of the corner of classroom

Clearly, for the data acquired at the corner of the classroom, when the range is larger than 7m, the residuals will get higher than others while the variation of the data at that range is not that large. However, this value is still lower than the guaranteed accuracy 3cm of the specification of the scanner.

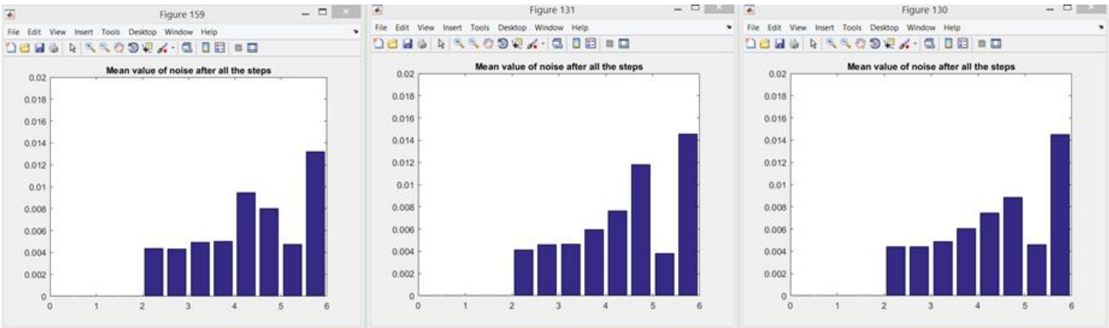

Figure 4- 21 Mean absolute values of residuals on range for data 2-1, 5-1, 10-1 of the center of classroom

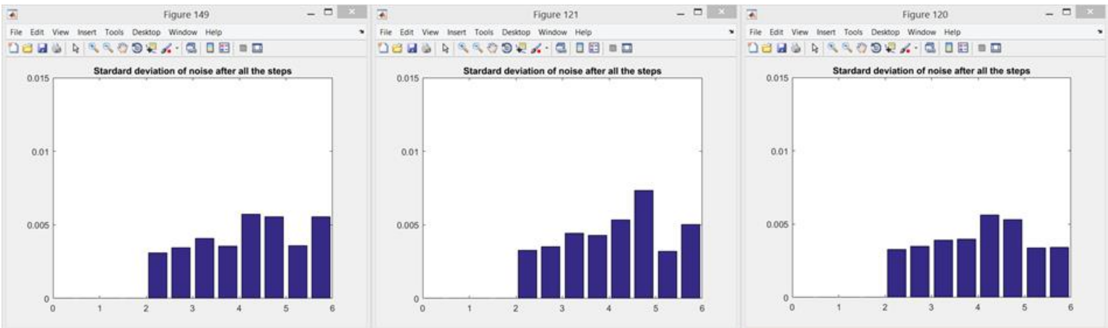

Figure 4- 22 Standard deviation of residuals on range for data 2-1, 5-1, 10-1 of the center of classroom

For the data acquired at the center of the classroom, there is no range of residuals that is clearly higher than others.

In order to see the accuracy of the standard deviation of the residuals, the number of points in each has been listed below.

Table 4- 14 The number of points in each interval in 2 datasets

	Data acquired at the corner	Data acquired at the center
1-1.5	216	0
1.5-2	73	0
2-2.5	57	127

2.5-3	392	68
3-3.5	0	124
3.5-4	0	44
4-4.5	60	17
4.5-5	4	21
5-5.5	23	76
5.5-6	0	11
6-6.5	5	0
6.5-7	43	0
7-7.5	13	0

The numbers of points which are larger than 0 but less than 20 have been labeled red. The number of points in those ranges may influence the accuracy of the standard deviation and mean absolute value in those ranges. But for both data, the residuals on every range are less than the guaranteed accuracy 3 cm.
Therefore I conclude that there is no strong relationship between range and residuals after the calibration, however, the accuracy may drop when the range is larger than 7 m, but that won't have huge influence on the overall accuracy.

4.7.2 Accuracy over time

4.7.2.1 Warm-up and over-heating problem

The RMS values and the calibration parameters are analyzed in this step using the data acquired at first minute, time with 5 minutes interval and 20th minute.
For data acquired at the corner of the classroom:
The points on each scan have been labeled manually like this.

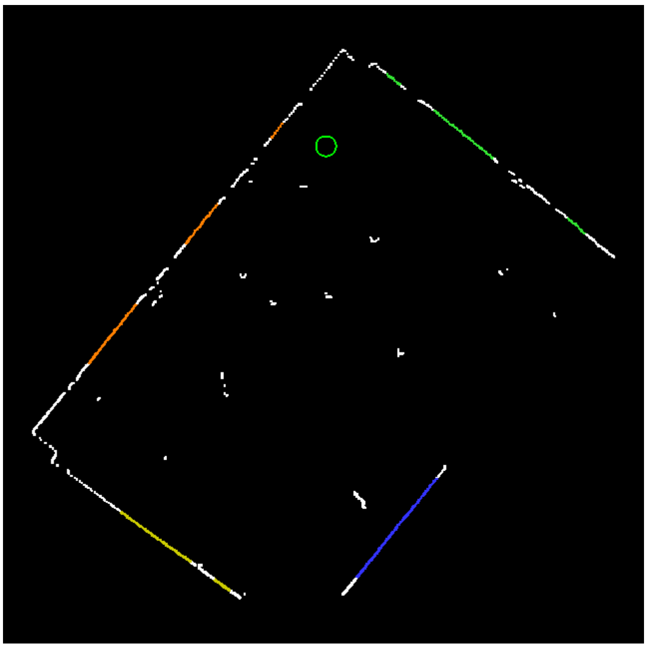

Figure 4- 23 Labeling data acquired at the corner

This is the table of RMS and RMS on range for the scan of 1st minute, 5 minutes interval and last minute.

Table 4- 15 RMS and parameters of calibration model for dataset acquired at corner

	1-1	2-1	5-1	10-1	15-1	20-1	20-2500
RMS(m)	0.0059	0.0059	0.0061	0.0065	0.0062	0.0068	0.0062
RMS range(m)	0.0082	0.0077	0.0082	0.0086	0.0082	0.0090	0.0081
k	1.0013	1.0011	1.0018	1.0020	1.0008	1.0015	1.0010
i	-0.0243	-0.0218	-0.0255	-0.0256	-0.0202	-0.0230	-0.0229

The table below shows the difference between RMS and RMS range of the data in 5 minute interval.

Table 4- 16 Changes in RMS and RMS on range for dataset acquired at corner

Differences	1~2	2~5	5~10	10~15	15~19	19~20
RMS (mm)	0	0.2	0.4	-0.3	0.4	-0.6
RMS range (mm)	-0.5	0.5	0.4	-0.4	0.8	-0.9

For the data acquired at the center:
The points on each scan have been labeled manually like this.

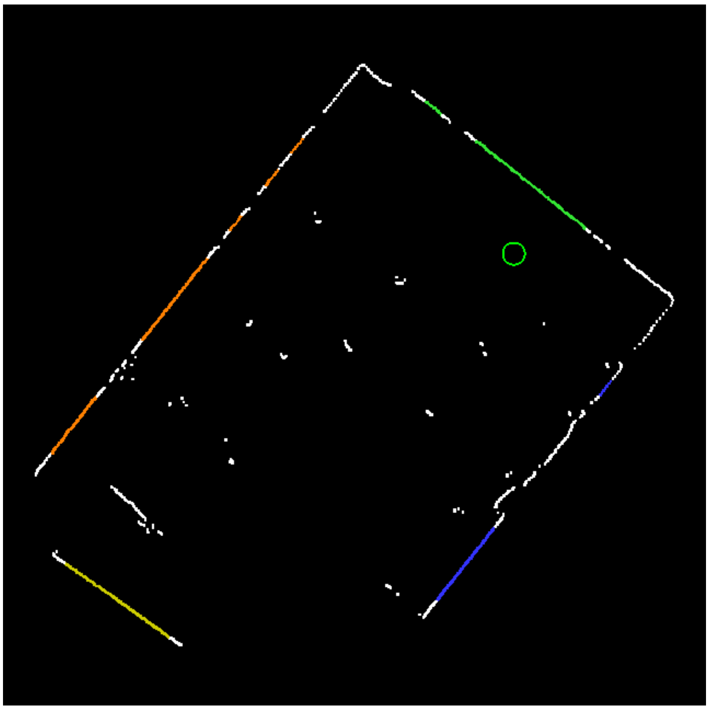

Figure 4- 24 Labeling data acquired at the center

Table 4- 17 RMS and parameters of calibration model for data acquired at the center

	1-1	2-1	5-1	10-1	15-1	20-1	20-2500
RMS(m)	0.0054	0.0058	0.0060	0.0059	0.0061	0.0058	0.0056
RMS range(m)	0.0061	0.0066	0.0069	0.0067	0.0071	0.0066	0.0065
k	1.0016	1.0021	1.0027	1.0026	1.0030	1.0022	1.0035
i	-0.0253	-0.0269	-0.0276	-0.0271	-0.0286	-0.0268	-0.0308

Table 4- 18 Changes in RMS and RMS on range for data acquired at the center

Differences	1~2	2~5	5~10	10~15	15~19	19~20
RMS (mm)	0.4	0.4	-0.1	0.2	-0.3	-0.4
RMS range (mm)	0.5	0.3	-0.2	0.4	-0.5	-0.1

There are changes in the RMS values for both data, but they are very small changes. And the values for the calibration parameter scale k and offset i remain stable in all the measurement, which are approximately 1.0010 and -0.0250.

I can conclude that

1. There is no warm-up time for this scanner, the scanner can start recording the data once we plug in.
2. In the first 20 minutes, the accuracy won't be influenced by the heating of the processor of the scanner, despite the scanner is hotter than the beginning.

4.7.2.2 Over longer time

The previous data was acquired on 15-Dec-2015, there was also dataset acquired on 07-Dec-2015 which is used to analyze if we need to calibrate the scanner again after not using it for long time. To compare the data, I chose the data acquired at 1st minute at the center on 15-Dec-2015 and 1st minute at the center on 07-Dec-2015, so the only variable is the date when the data is acquired.

Table 4- 19 Comparison between data acquired on 2 different dates

	Dataset acquired on 15-Dec-2015	Dataset acquired on 07-Dec-2015
RMS (m)	0.0054	0.0057
RMS on range (m)	0.0061	0.0066
k	1.0016	1.0011
i	-0.0253	-0.0217

From the table above we can see that the RMS values didn't change a lot, the values of scale parameter k and offset parameter i remain judging by the 2 datasets.

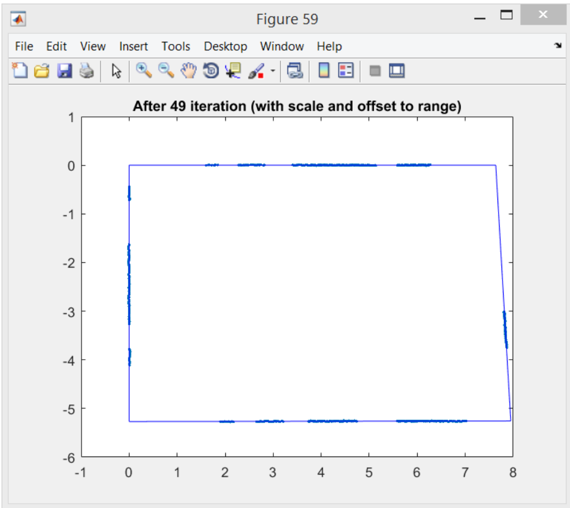

Figure 4- 25 Plot of calibrated scanner with data acquired on earlier time

The plot also indicates that the calibration model has successfully calibrated the scanner.

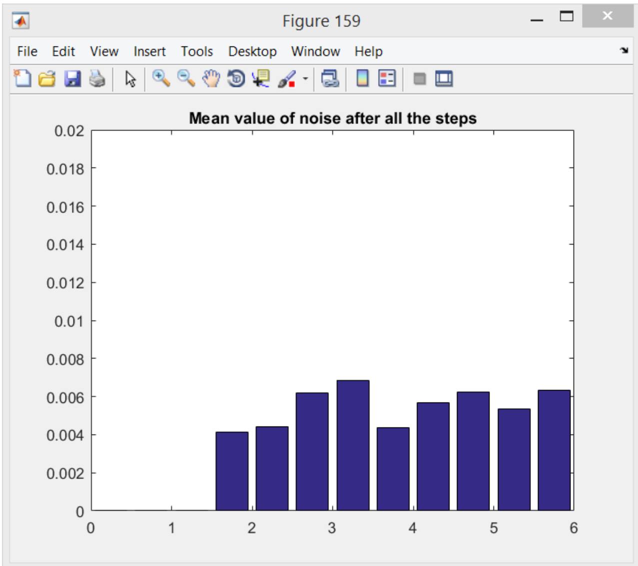

Figure 4- 26 Mean value of residual after calibration in dataset acquired earlier

The mean absolute values of the residual after the calibration are way below the guaranteed accuracy of the specification of the laser scanner.
In conclusion, there is no need to calibrate the scanner after not using it for 8 days.

5 EVALUATION AND DISCUSSION

5.1 Evaluation

In this chapter, the accuracy of the calibration model and the complexity of computation have been investigated.

5.1.1 Accuracy

The RMS and RMS on range values are used to evaluate the accuracy of the scanner.

Table 5- 1 RMS values of data acquired at the corner of classroom

	1-1	2-1	5-1	10-1	15-1	20-1	20-2500
RMS(m)	0.0059	0.0059	0.0061	0.0065	0.0062	0.0068	0.0062
RMS range(m)	0.0082	0.0077	0.0082	0.0086	0.0082	0.0090	0.0081

Table 5- 2 RMS values of data acquired at the center of classroom

	1-1	2-1	5-1	10-1	15-1	20-1	20-2500
RMS(m)	0.0054	0.0058	0.0060	0.0059	0.0061	0.0058	0.0056
RMS range(m)	0.0061	0.0066	0.0069	0.0067	0.0071	0.0066	0.0065

One thing to notice is that the RMS values for the data acquired at the corner is approximately 2mm higher than the RMS values for the data acquired at the center of the classroom. This is because for the data acquired at the corner of the classroom, there are data whose range is larger 7m, where could be larger residuals than others as mentioned in 4.8.1, which led to the higher RMS values.

The RMS values are much lower than the guaranteed accuracy of the specification of the scanner (3 cm).

5.1.2 Computational complexity

Except the pre-process data has been carried out in Point Cloud Mapper (PCM), the rest of the program is written in Matlab R2015b.

PCM requires manual labeling the points with the corresponding walls, which needs to be done carefully and label for each dataset.

The program written in Matlab runs fast except for the part where to calculate the residuals on range, which takes most of time due to involvement of equation solving in that part.

5.2 Discussion

In this part, I discussed the methods of data acquirement, calculation of parameters and the proposed calibration model.

5.2.1 Discussion on data acquirement

The reference data acquiring method described in 3.2.2 is clearly better than measuring the walls directly in theory because in reality there are angles influencing the measurement of walls, which are very hard to measure accurately.

The data acquired by the laser scanner has provided sufficient data to form the calibration model.

Also, the accuracy over range and the accuracy over time have successfully been analyzed because the data was acquired at different ranges during 20 minutes. In addition, 2 data collection using the same laser scanner with an 8-day gap allows analyzing if recalibration is needed after not using the laser scanner for long time. However, the maximum range is 7.5m, so if the calibration model still works when the range is larger than 7.5m cannot be determined.

5.2.2 Discussion on method of calculation of parameters

The accurate values of parameters are calculated using least square after iterations. Least square can minimize the sum of the squares of the errors of every equation, at each iteration the system is approximated by a linear one (Wikipedia, 2016). The calculation using least square has been proven to be effective and accurate judging by the RMS values and plots.

5.2.3 Discussion on the proposed calibration model

The proposed calibration model is $\hat{r} = k * r + i$, it has

1. Successfully calibrate the scanner, making it way below the guaranteed accuracy of the specification of laser scanner.
2. Very close values of the calibration parameter for the different data acquired by the same scanner.

6 CONCLUSION

6.1 Conclusions

The objective of my research is to calibrate the laser scanner Hokuyo UTM-30LX. It has 5 steps: step 1 is pre-process data, in where the reference data has been calculated and the laser data has been labeled. Step 2 is calculation of rotation and location of the scanner, in where the accurate values of rotation of the scanner β, location of the scanner in the model coordinate system (X_0,Y_0) have been calculated using least square. Step 3 is calculation of added parameter scale, the newly added parameter scale has been calculated along with its values of rotation of the scanner β, location of the scanner in the model coordinate system (X_0, Y_0). Step 4 is calculation of added parameter offset, in where the newly added parameter offset, the scale parameter, values of rotation of the scanner β, location of the scanner in the model coordinate system (X_0, Y_0) have been calculated. The last step is to analyze the accuracy over range and accuracy over time after the calibration.

The accuracy of the scanner after the calibration is below the guaranteed accuracy described in the specification of the laser scanner.

So I can make the following conclusions regarding the scanner based on the results:

1. The calibration model has improved the accuracy of the scanner.
2. The accuracy of the scanner is a little compromised when the range of the scanner exceeds 7 meters, but it is still way below the guaranteed accuracy 3cm.
3. The scanner doesn't have a warm-up or overheating problem (when using this scanner less than 20 minutes).
4. There is no need to recalibrate the laser scanner after 8 days not using it.

6.2 Answers to the research questions.

1. What is an appropriate indoor environment for calibration and how to determine if the scanner needs calibration?

   The appropriate indoor environment should be the one that can be mathematically described.

   The calibration can improve the accuracy of a laser scanner, so when using a scanner for highly-accurate measurement, the scanner should be calibrated.
2. What is the optimal mathematical model to calibrate the scanner?

   The proposed calibration model is $\hat{r} = k * r + i$, where k is the scale parameter and i is the offset parameter for the range. This calibration model has successfully reduced the residuals a lot and there are no larger systematic errors in the remaining residuals.
3. How does the accuracy change with the range?

   The accuracy is only been compromised when the range exceeds 7 meters, but it is still way below the guaranteed accuracy.
4. Is the calibration model stable? Are the values for the parameters stable or should I calibrate the scanner every time I use this?

   Yes, the calibration model is stable in the first 20 minutes. There is no warm-up or overheating problem. Also, there is no need to recalibrate the laser scanner after 8 days not using it.

There is no need to calibrate the scanner every time use it.

5. How to evaluate the noise after calibration?

   The noise has been evaluated using accuracy over range and accuracy over time.

6.3 Recommendations

There are 3 recommendations regarding the data acquirement and calibration parameters determination for the research.

1. The laser scanner can be running for longer time to see if there are larger residual when the using time is longer, however, this may lead to problems like too much data.
2. The maximum range for the data is 7.5m, we still cannot determine what effects may have for data with range larger than 7.5m. So it will be better if we acquire that data in larger room.
3. The chosen environment can be more rectangular if applicable.
4. Despite the accuracy after calibration has been clearly improved, there is still pattern may be analyzed so that the new calibration parameters may be added, like there still is a pincushion distortion if we look at the plot. The similar parameters may be added like in the model raised by Mader et al in 2014 described in section 2.3.2.

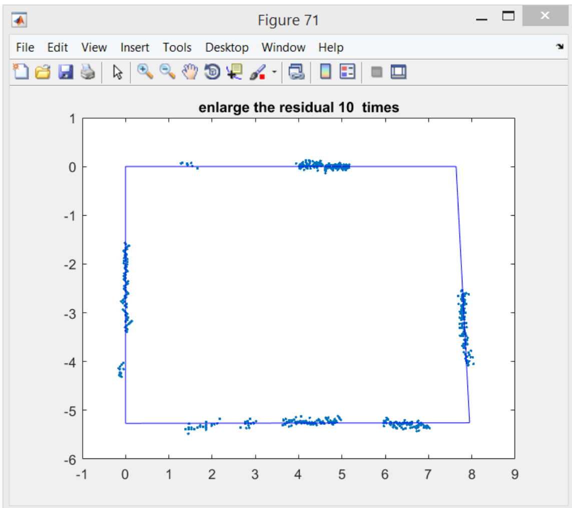

Figure 6- 1 Enlargement of residual 10 times for data 5-1 of the center of classroom

LIST OF REFERENCES

Biber, P., Biber, P., Andreasson, H., Andreasson, H., Duckett, T., Duckett, T., … Others. (2004). 3D modeling of indoor environments by a mobile robot with a laser scanner and panoramic camera. *IEEE/RSJ Int. Conf. on Intel. Rob. Sys*, 3430–3435.

Doxygen.(2015).Lens Distortion. Retrieved 27 January 2016, from http://www.aqsense.com/docs/docu/lensDistortion.html

Glennie, C., & Lichti, D. D. (2010). Static calibration and analysis of the velodyne HDL-64E S2 for high accuracy mobile scanning. *Remote Sensing*, *2*(6), 1610–1624. http://doi.org/10.3390/rs2061610

Henry, P., Krainin, M., Herbst, E., Ren, X., & Fox, D. (2012). RGB-D Mapping : Using Depth Cameras for Dense 3D Modeling of Indoor Environments. *The International Journal of Robotics Research*, *31*(5), 647–663. http://doi.org/10.1177/0278364911434148

Jain, S., Nandy, S., Chakraborty, G., Kumar, C. S., Ray, R., & Shome, S. N. (2011). Error modeling of Laser Range Finder for robotic application using time domain technique. *2011 IEEE International Conference on Signal Processing, Communications and Computing (ICSPCC)*, 1–5. http://doi.org/10.1109/ICSPCC.2011.6061771

Khoshelham, K., & Elberink, S. O. (2012). Accuracy and Resolution of Kinect Depth Data for Indoor Mapping Applications. *Sensors*, *12*(12), 1437–1454. http://doi.org/10.3390/s120201437

Kim, J. B., & Kim, B. K. (2011). Efficient calibration of infrared range finder PBS-03JN with scan-wise cubic hermite splines for indoor mobile robots. *URAI 2011 - 2011 8th International Conference on Ubiquitous Robots and Ambient Intelligence*, 353–358. http://doi.org/10.1109/URAI.2011.6145995

Kneip, L., Tâche, F., Caprari, G., & Siegwart, R. (2009). Characterization of the compact Hokuyo URG-04LX 2D laser range Scanner. *Proceedings - IEEE International Conference on Robotics and Automation*, 1447–1454. http://doi.org/10.1109/ROBOT.2009.5152579

Hokuyo Ltd, (2012). Scanning Laser Range Finder UTM-30LX/LN Specification. Retrieved 15 January 2016, from http://www.hokuyo-aut.jp/02sensor/07scanner/download/products/utm-30lx/

Mader, D., Westfeld, P., & Maas, H.-G. (2014). An Integrated Flexible Self-calibration Approach for 2D Laser Scanning Range Finders Applied to the Hokuyo UTM-30LX-EW. *ISPRS - International Archives of the Photogrammetry, Remote Sensing and Spatial Information Sciences*, *XL-5*(June), 385–393. http://doi.org/10.5194/isprsarchives-XL-5-385-2014

Okubo, Y., Ye, C., & Borenstein, J. (2009). Characterization of the Hokuyo URG-04LX laser rangefinder for mobile robot obstacle negotiation. *Proceedings of SPIE*, *7332*, 733212:1–733212:10. http://doi.org/Artn 733212\nDoi 10.1117/12.818332

Sheehan, M., Harrison, a., & Newman, P. (2012). Self-calibration for a 3D laser. *The International Journal of Robotics Research*, *31*(5), 675–687. http://doi.org/10.1177/0278364911429475

Surmann, H., Nüchter, A., & Hertzberg, J. (2003). An autonomous mobile robot with a 3D laser range finder for 3D exploration and digitalization of indoor environments. *Robotics and Autonomous Systems*, *45*(3-4), 181–198. http://doi.org/10.1016/j.robot.2003.09.004

Vosselman, G. (2014). Design of an indoor mapping system using three 2D laser scanners and 6 DOF SLAM. *ISPRS Annals of Photogrammetry, Remote Sensing and Spatial Information Sciences*, *II-3*(September), 173–179. http://doi.org/10.5194/isprsannals-II-3-173-2014

Vosselman, G., & Maas, H.-G. (2010). *Airborne and terrestrial laser scanning:* . Whittles Publishing. Retrieved from https://www.dawsonera.com:443/abstract/9781849950138

Wikipedia. (2016). Simple linear regression. Retrieved 26 January 2016, from https://en.wikipedia.org/wiki/Least_squares

Ye, C. Y. C., & Borenstein, J. (2002). Characterization of a 2D laser scanner for mobile robot obstaclenegotiation. *Proceedings 2002 IEEE International Conference on Robotics and Automation (Cat. No.02CH37292)*, *3*(May). http://doi.org/10.1109/ROBOT.2002.1013609